

**N 7 3 - 2 0 7 3 5**

**NASA TECHNICAL  
MEMORANDUM**

NASA TM X- 68207

NASA TM X- 68207

**CASE FILE  
COPY**

**EXPERIMENTAL DETAILED POWER DISTRIBUTION IN A FAST  
SPECTRUM THERMIONIC REACTOR FUEL ELEMENT AT THE  
CORE/BeO REFLECTOR INTERFACE REGION**

by Paul G. Klann and Edward Lantz  
Lewis Research Center  
Cleveland, Ohio 44135  
March 19, 1973

## ABSTRACT

A zero-power critical assembly was designed, constructed, and operated under two previous NASA-funded programs for the purpose of conducting a series of benchmark experiments dealing with the physics characteristics of a UN-fueled,  $\text{Li}^7$ -cooled, Mo-reflected, drum-controlled compact fast reactor for use with a space-power conversion system (see NASA-CR-72820 and AI-72-33). The critical assembly was modified to simulate a fast spectrum advanced thermionics reactor by (1) using BeO as a reflector in place of some of the existing molybdenum, (2) substituting Nb-1Zr tubing for some of the existing Ta tubing, and (3) inserting four full-scale mockups of thermionic type fuel elements near the core and BeO reflector boundary. These mockups were surrounded with a buffer zone having the equivalent thermionic core composition. In addition to measuring the critical mass of this thermionic configuration, a detailed power distribution in one of the thermionic element stages in the mixed spectrum region was measured. A power peak to average ratio of two was observed for this fuel stage at the midplane of the core and adjacent to the reflector. Also, the power on the outer surface adjacent to the BeO was slightly more than a factor of two larger than the power on the inside surface of a 5.08 cm (2.0 in.) high annular fuel segment with a 2.52 cm (0.993 in.) O.D. and a 1.86 cm (0.731 in.) I.D.

## FOREWORD

The experimental and critical assembly work described herein was performed by Atomix International, a Division of North American Rockwell Corporation, under Contract NAS3-16816, with Mr. Paul G. Klann, Nuclear Systems Division, NASA Lewis Research Center, as Project Manager. The thermionic reactor mockup design and data evaluation was done by Paul G. Klann and Edward Lantz. This work represents a continuation of a program which was reported in NASA-CR-72820 under Contract NAS3-12982 and of a program which was reported in AI-72-33 under Contract NAS3-14421.

The contribution of W. H. Heneveld, T. H. Springer, V. A. Swanson, and R. J. Tuttle at Atomix International in performing the critical experiments and reducing the data is gratefully acknowledged.

# CONTENTS

	Page
FORWARD. . . . .	
ABSTRACT . . . . .	
SUMMARY. . . . .	1
I. INTRODUCTION . . . . .	1
A. Background . . . . .	1
B. Scope of the Present Program . . . . .	2
C. Purpose of the Current Work. . . . .	2
II. DESCRIPTION OF THE THERMIONICS CRITICAL ASSEMBLY. . . . .	2
A. Basic Critical Assembly. . . . .	2
B. Modified Critical Assembly . . . . .	4
(1) Alterations to Reactor . . . . .	4
(2) Accuracy of Geometrical Simulation of the Thermionic Core . . . . .	6
C. Simulated Thermionic Fuel Elements . . . . .	6
(1) Description. . . . .	6
(2) Accuracy of the Thermionic Fuel Element Simulation . .	7
D. Thermionic Mockup Buffer Region. . . . .	8
(1) Description. . . . .	8
(2) Accuracy of the Buffer Region Simulation . . . . .	9
E. Driver Region. . . . .	9
III. EXPERIMENTAL METHODS . . . . .	10
A. Introduction . . . . .	10
B. Measurement of Drum Worth. . . . .	10
C. Measurement of the All-Drums-In Excess Reactivity. . . .	11
D. Measurement of Critical Mass . . . . .	11
E. Measurement of Power Distribution. . . . .	11
F. Units of Measure . . . . .	12
IV. EXPERIMENTAL RESULTS. . . . .	12
A. Excess Reactivity. . . . .	12
B. Critical Mass. . . . .	13
C. Drum Worth . . . . .	13
D. Power Distribution . . . . .	13
(1) Foil Counting. . . . .	13
(2) Film Exposure. . . . .	14
E. Fuel Element Substitution. . . . .	15
V. DISCUSSION OF RESULTS. . . . .	15
A. Experimental . . . . .	15
B. Analytical . . . . .	16
VI. CONCLUSION. . . . .	16
APPENDIX A - CHEMICAL IMPURITIES IN CORE MATERIALS . . . . .	17

EXPERIMENTAL DETAILED POWER DISTRIBUTION IN A FAST SPECTRUM  
THERMIONIC REACTOR FUEL ELEMENT AT THE CORE/BeO REFLECTOR  
INTERFACE REGION

by Paul G. Klann and Edward Lantz

SUMMARY

A zero power critical assembly was designed and constructed in order to study the reactivity characteristics of a UN-fueled,  $\text{Li}^7$ -cooled, Mo-reflected, drum-controlled compact fast reactor for use with a space power conversion system.<sup>1,2</sup> For the present investigation, one-half of this critical assembly was reconfigured to simulate the core-pressure vessel-reflector interface of the advanced 100 kwe General Atomic Nuclear Electric Propulsion thermionic reactor concept in order to measure the power distribution at the interface of the fast spectrum core and the thermalizing BeO reflector.

The power distribution around and within an axially centered mock-up test thermionic fuel element stage at the core-pressure vessel-reflector interface was measured by activating and counting a tightly wound coil of 0.0076 cm (0.003 in.) highly enriched U-235 foil. This coil was a simulation of the annular fuel stage of the concept.

Backing the mockup test element at the core-reflector interface were three additional mockup thermionic fuel elements clustered on the thermionic lattice spacing, and a buffer region extending to the center of the critical assembly. This buffer region was composed of or alloy rods, tungsten and tantalum wires in Nb-1% Zr tubing combined so that the average volume fractions of the thermionic reactor concept were achieved. The remainder of the critical assembly was used as a driver region and was loaded to criticality using or alloy in aluminum tube fuel elements.

The power distribution data obtained for a mockup thermionic fuel stage located at the midplane of the core and adjacent to the BeO reflector indicated a power peak-to-average ratio of two. The measurements indicate that a power peaking factor of this large magnitude for the fuel stages exist at the core-reflector regions and its effects must be incorporated in the thermionic concept core design studies.

I. INTRODUCTION

A. Background

In 1969, the National Aeronautics and Space Administration Lewis Research Center initiated a series of critical experiments in connection with the design of a small, compact, fast reactor for space application.

A critical assembly was designed, built, and operated for this purpose by Atomics International, and an extensive experimental program was conducted (see refs. 1 and 2). Recently the Lewis Research Center undertook a review of some of the current thermionics reactor development problems and identified the need for a series of experiments dealing with the power peaking that occurs in fuel elements located at the core boundary of a fast spectrum core, BeO-reflected, advanced thermionic reactor concepts. The existing critical assembly was therefore modified in such a way that a portion of the core simulated the composition, and, partially, the geometrical layout of a reference thermionic reactor. A detailed experimental measurement of this power peaking in a thermionic fuel element was subsequently carried out.

### B. Scope of the Present Program

In addition to modifying the existing critical assembly to provide a good partial simulation of an advanced thermionics reactor, the scope of the present program consisted of determining the critical mass of the modified core, and of carrying out the detailed power distribution measurement at the fast core-BeO reflector interface. Auxiliary experiments were conducted to determine the reactivity worth of a control drum and the reactivity change of substituting the previously used Ta-Li<sup>7</sup><sub>3</sub>N fuel elements for the aluminum elements in the driver region of the thermionics critical.

### C. Purpose of the Current Work

The purpose of the Thermionic Mockup Critical Experiment is to obtain data concerning the power distribution around and within a thermionic fuel element (TFE) located at the edge of the core-reflector interface of the present thermionic reactor design. The importance of these measurements is that they will yield information on the power distribution at the mixed spectrum interface of a fast spectrum core and a thermalizing BeO reflector in a realistic simulation of the TFE-reflector region.

## II. DESCRIPTION OF THE THERMIONICS CRITICAL ASSEMBLY

### A. Basic Critical Assembly

The critical assembly that was in use, prior to the initiation of this program is depicted in figure 1 and is described in detail in references 1 and 2. The assembly was composed of a close-packed star-shaped array of 181 fuel elements surrounded radially by six massive Mo reflectors (see Figure 2). Imbedded in the radial reflector region and also partly in the core region (between the points of the star) were six symmetrically located cylindrical control drums whose axes

were parallel to the axis of the core. Each control drum contained 11 fuel elements and a molybdenum reflector, and was backed by a massive Ta absorber segment. In order to provide a rapid-acting safety device mechanism for the reactor, four of the six radial Mo reflector pieces were capable of falling away from the core (scramming) and thereby producing a substantial reduction in reactivity. This scram system consisted of two independent and diametrically opposed safety elements to each of which were attached two of the Mo reflectors in a ganged fashion.

In the shutdown condition, four reflectors were located away from the core and all six control drums are rotated such that the Ta absorber segment in each drum was in the core region and the drum fuel elements were facing away from the core.

In order to achieve criticality, the four reflectors were raised into position (adjacent to the core) by the safety element drive motors and then the control drums were sequentially "driven in"; i.e., rotated to bring fuel into the core.

Surrounding the massive Mo reflectors were four Ta segments. One segment was located on each of the two fall-away safety-element systems and one on the outside of each of the two stationary reflectors. The segments had an outside radius of 29.23 cm (11.51 in.), a thickness of 0.691 cm (0.272 in.) and a height of 59.7 cm (23.5 in.). During reactor operation, when the reflectors were in the up-position, the four Ta segments formed a cylindrical shell completely enclosing the reactor on the lateral surface.

Dimensionally, the critical assembly was 56.845 cm (22.38 in.) high, including upper and lower axial reflectors, and 57.15 cm (22.5 in.) in diameter, including the massive radial reflectors. The core proper was 37.508 cm (14.767 in.) high and had a "diameter" of 38.33 cm (15.09 in.) as measured from the centerline of one fuel element at a point of the star to the centerline of a diagonally opposite fuel element at the point of the star.

Inside the Ta pressure vessel mockup segments were the massive Mo reflectors. Each of the six reflectors was about 60.2 cm (23.7 in.) high and had an outside radius of 28.60 cm (11.26 in.). The thickness from the outer radius to the nearest fuel element was 8.20 cm (3.23 in.). The reflectors had circular cutouts for accommodating the rotatable control drums and therefore wrapped around the drums to some extent. However, in order to allow four of the reflectors to fall away from the core, a portion of these four reflectors was cut away so that they "cleared" the drums. Four small triangular Mo filler pieces were therefore installed in the stationary core in such a way that, when all reflectors were in the up-position, they were, for all practical purposes, identical.

Located within the region occupied by these massive Mo reflectors and the six control drums was the star-shaped stationary core. The

small circles shown in figure 2 represent some of the 181 fuel elements that made up the core proper. The locations of the center line of the remainder of the core elements are shown by an "X" in the figure. The fuel elements were 59.941 cm (23.599 in.) high, were 2.159 cm (0.850 in.) in outside diameter, and located on a 2.215-cm (0.872-in.) lattice pitch.

Six additional triangular-shaped Mo pieces, apart from the four noted above, were placed in the core to fill up the void space that existed between the hexagonal array of honeycomb tubes and the control drums. A cross sectional view of the core as produced by a vertical section formed by passing a plane through the axis of the core and the axis of a control drum is drawn in the right-hand half of the center-line of the drawing of Figure 3. The left half of the figure is the view that would be seen along a section formed by passing a plane through the axis of a fuel element at the point of the star. To provide an indication of the relative positions of the fuel element components to the other core components, an outline of one fuel element is depicted in the figure.

The axis of each of the six control drums was parallel to the axis of the core and located on a 20.917-cm (8.235-in.) radius. The speed of rotation, both for the case in which fuel is going into the core and the case in which fuel is going out, was low (about 0.12 rpm). The detailed layout of the control drum is shown in cross sectional view at the drum midplane in Figure 4. The main structural member of the drum was the massive Mo reflector piece to which an upper and lower drum grid plate was attached. This Mo piece was 60.2 cm (23.7 in.) high (the effective height of the control drum). Each drum normally had a Ta absorber segment which was also 60.2 cm (23.7 in.) high.

On one side of the drum was a region which contained a group of fuel elements identical to those in the stationary portion of the core. Since the void fraction in this region was rather high with fuel elements alone, several round Mo filler rods were inserted. All of these rods were 60.2 cm (23.7 in.) high, but varied in diameter, as indicated in the figure. In addition to the round rods, a large trapezoidal-shaped filler piece 60.2 cm (23.7 in.) high, was also utilized to fill the gap between the Mo reflector segment and the inner ring of the honeycomb tubes.

## B. Modified Critical Assembly

### (1) Alterations to Reactor

The reactor, as described above, was modified for the current program in the manner depicted on Figure 5. This portion of the figure shows, in solid lines, the modified assembly and also indicates, in dashed lines, the former locations of some of the previously existing components. In addition to alterations in the overall reactor configuration, the active core was divided into three regions: a driver region



that consists of fuel elements made up of aluminum tubing, a buffer region that consists of five different sizes of fuel elements (four using Nb-1Zr as a structural material and one using aluminum), and a thermionic fuel element (TFE) region that consists of four large diameter Nb-1Zr tubes containing fuel and a simulator of the tungsten emitter in an actual TFE.

With regard to the overall reactor configuration, the following modifications were made:

(1) Drums 1, 2, and 3 were completely removed. (See Figure 2 for drum locations).

(2) Fuel elements in Positions 6-4 through 6-13, 7-3 through 7-10, 8-3 through 8-8, 9-2 through 9-5, and 10-2 and 10-3, inclusive, were withdrawn. (See Figure 6 for fuel element locations).

(3) The two massive molybdenum reflectors and the tantalum pressure vessel mockup, all of which were previously mounted on the scram mechanism adjacent to Drums 1, 2, and 3, were removed.

(4) Each of the two tantalum pressure vessel mockups located outside of the stationary radial Mo reflectors was extracted.

(5) Two aluminum canisters, each containing 240 half-hexagons of BeO [each nominally 2.063 cm (0.8125 in.) across the parallel sides and 14.288 cm (5.625 in.) long] and 396 cylinders of BeO each 1.05 cm (0.415 in.) in diameter by 2.54 cm (1.0 in.) long, were mounted on the scram mechanism as shown in Figure 7. Also, within each canister were placed two Nb-1Zr sheets so oriented that they formed a slab 0.241 cm (0.095 in.) thick by 57.15 cm (22.50 in.) high by 16.88 cm (6.567 in.) wide. (See Figure 7.) The effective cross sectional shape of each BeO scrammable reflector, as viewed in the core midplane, was a trapezoid 10.31 cm (4.06 in.) thick by 16.68 cm (6.567 in.) wide on the face adjacent to the core. The height of the BeO reflector was 57.15 cm (22.50 in.), as constituted by stacking four half-hexagons end-to-end. Axially the BeO reflector was centered about the core midplane. Since the cylindrical columns of BeO were shorter than the columns of half-hexagons, an aluminum spacer was located under the cylindrical columns in order to position them symmetrically about the core midplane.

(6) One stationary side-BeO reflector, having a cross sectional shape of a parallelogram in the core midplane, was located adjacent to each of the two stationary Mo reflectors. This BeO reflector was formed by placing two half-hexagons side by side. Thus, a total of eight BeO half-hexagons was required to form a 57.15 cm (22.50 in.) high zone for each side reflector. A 55.9 cm (22.0 in.) high column of BeO circular cylinders identical to those used in the scrammable reflector system will also be added to each side reflector system as indicated in Figure 7. Figure 5 indicates the mounting technique for these side reflectors (Section B-B). These reflectors were also centered axially about the core midplane.

(7) In order to accommodate a BeO reflector in the central position adjacent to TFE No. 4, four BeO half-hexagons were machined to reduce their widths across the base and top. The distance across the flats of each BeO half-hexagon remained the same; i.e., 2.063 cm (0.8125 in.), nominally. The widths of the base and top of the modified half-hexagons of BeO were 4.161 cm (1.638 in.) and 1.778 cm (0.700 in.), respectively. A 55.9 cm (22.0 in.) high column of BeO circular cylinders, identical to those used in the scrammable-reflector system, was also added to the central reflector canister, and all BeO was centered about the core midplane.

## B. Modified Critical Assembly

### (2) Accuracy of Geometrical Simulation of the Thermionic Core

Figure 8 shows a plan view of the General Atomic 100 kwe Nuclear Electric Propulsion reference reactor design. The core-pressure vessel-reflector interface of this reference design was simulated in the critical assembly. The simulation is shown in Figure 9 drawn to scale. It is seen that the interface between the core and the BeO reflector in the reference design is essentially the chord of a circle. This was simulated by a BeO slab made up of trapezoidal BeO pieces. The semi-circular BeO rod within the pressure vessel to the left of fuel element No. 1 was simulated by a BeO trapezoid and a BeO rod. The pressure vessel was represented by a 0.241 cm (0.095 in.) Nb-1% Zr plate abutting the BeO slab, such that the pressure vessel mockup in simulation is in the correct proximate position relative to test fuel element No. 1, Figure 8.

An overlay of Figure 9 on Figure 8 is shown in Figure 10. A close geometrical simulation of the reference core-pressure vessel-reflector is apparent and it is noted that the simulation is especially accurate in the vicinity of the test element.

## C. Simulated Thermionic Fuel Elements

### (1) Description

The core region was also modified to produce a simulation of a thermionic reactor. In particular, four elements that simulated the current thermionic fuel element (TFE) design were inserted into the core at the positions indicated in Figure 7. The design of the TFE mockups is shown in Figure 11. The main structural member of the mockup is a 3.31 cm (1.300 in.) O.D. by 0.203 cm (0.080 in.) wall by 59.27 cm (23.336 in.) long Nb-1Zr tube with special cups at each end which serve to locate the mockup in an upper and lower auxiliary grid plate. These auxiliary grid plates, shown in outline in Figure 7, were required since the TFE mockups would not fit into the regular grid pattern of the previous core. Within each of the four Nb-1Zr tubes and at the core midplane was placed a tungsten cup, each nominally 2.731 cm

(1.075 in.) in outside diameter and having a wall thickness of 0.102 cm (0.040 in.) and a height of 5.08 cm (2.00 in.). Within each of the tungsten cups was placed a coil of fully-enriched uranium foil that was 0.0076 cm (0.003 in.) thick and weighed 200 gms. The outside diameter of the coil corresponded to the inside diameter of the tungsten cup and the height of the coil was 4.92 cm (1.938 in.). The inside diameter of the coil was approximately 1.86 cm (0.731 in.). Within the coil of fuel was located a cylindrical rod of teflon approximately 4.92 cm (1.938 in.) high and 1.78 cm (0.70 in.) in diameter. The teflon provided carbon atoms which, in conjunction with the uranium foil, simulated the UC fuel in the reference TFE.

Above and below the tungsten cup were placed 0.431 cm (0.170 in.) diameter by 15.64 cm (6.00 in.) long fully-enriched uranium rods, 0.457 cm (0.180 in.) diameter by 15.64 cm long W rods, 0.279 cm (0.110 in.) diameter by 15.64 cm long Ta wire, and 0.152 cm (0.060 in.) diameter by 15.64 cm long fully-enriched uranium wires in the quantities depicted in Figure 11. These materials were confined to the annular space between the Nb-1Zr structural tube and a smaller and shorter Nb-1Zr tube. A teflon filler rod approximately 1.56 cm (0.625 in.) in diameter by 15.64 cm long (6.1575 in.) was inserted into the inner Nb-1Zr tube at each end. Separating this upper and lower fuel region from the tungsten cup and simulating the structural and electrical connections in the reference TFE are two Nb-1Zr discs. These are dimensionally described in the figure.

One standard molybdenum reflector 10.0 cm (3.94 in.) long by 1.49 cm (0.588 in.) in diameter was placed within the small Nb-1Zr tube at each end of the element. In order to keep the fuel rods in place, an aluminum tube with an outside diameter of approximately 2.54 cm (1.0 in.) and an inside diameter of approximately 1.78 cm (0.70 in.) was also added at each end.

The overall length of the fueled region of the TFE mockup including the two Nb-1Zr discs that are above and below the tungsten cup corresponds to that in the rest of the core. The weight of all of the materials are listed in table I.

### C. Simulated Thermionic Fuel Elements

#### (2) Accuracy of the Thermionic Fuel Element Simulation

Figure 12 compares a half stage of the mockup fuel element with a half stage of the 100 kwe General Atomic Nuclear Electric Propulsion reactor fuel element. In the reference element stage, the fuel annulus is composed of a uranium-zirconium carbide composite containing 200 grams of U-235. This was simulated in the mockup by a 200 gram coil of highly enriched U-235 foil, 0.0076 cm thick (0.003 in.), such that the mockup annulus has the same optical thickness as the reference fuel annulus.

The carbon content of the reference composite was incorporated by a teflon ( $C_2F_4$ ) plug within the U-235 coil. The tungsten emitter was reproduced in the mockup by a tungsten cup of the same dimensions, while the electrode region between the fuel stages was taken into account by a Nb-1% Zr slab that contained the volume of Nb in the interstage region of the reference element.

Table II compares the volume fractions obtained in the simulation to those of the reference design in the thermionic fuel element (TFE) region above the test stage.

The above comparisons show that the TFE mockup is a close simulation to the reference configuration in all the important material and geometrical aspects of the design.

#### D. Thermionic Mockup Buffer Region

##### (1) Description

Since only four TFE mockups could be made to fit conveniently in the existing core space and still achieve criticality, a buffer region that, although it did not provide geometrical simulation of the reference TFE core, but which contained the required material quantities, was placed around the TFE mockups. The buffer region consisted of a total of 51 fuel elements, 39 of which were constructed of Nb-1Zr tubing and 12 of aluminum tubing.

The loading of these elements is indicated in table III. The fuel height was 31.51 cm (14.767 in.), with approximately 10 cm (3.94 in.) reflectors at each end. The designation of the positions of most of these elements followed the same pattern used in earlier cores since they occupied positions in the regular grid pattern. See Figure 7. Five buffer region elements were, however, located off the regular grid pattern. Their position designation was determined by the nearest regular lattice location. Thus, buffer region elements (2-5), (3-4), (4-5), (5-6), and (5-7) did not have normal lattice positions and were held in place by the two auxiliary grid plates (one at the top of the core and one at the bottom) which were 0.305 cm (0.120 in.) thick each. (The parentheses around the fuel position designations will be used to signify this asymmetry.) Incidentally, the auxiliary grid plates also held the center BeO reflector segment in place. The two plates were keyed to existing upper and lower grid plates by using two regular grid holes.

Teflon strips or sheets, 37.47 cm (14.75 in.) high by approximately 0.152 cm (0.069 in.) thick, were placed between the fuel elements in the buffer region in order to provide the simulation of the carbon content in the fuel of the advanced thermionic reference reactor.

As can be seen in table III, the 39 Nb-1Zr buffer elements consisted of four types (designated A, AA, B and C) that differed from one another primarily in the size of the tubing that was available to construct them. However, in the case of types A and AA, the only difference was the length of the tubing, the type AA element being used in positions (2-5), (3-4), (4-5), (5-6) and (5-7). The detailed descriptions of these four types of elements are given in Figure 13. In all types, the fuel cluster, which consisted of the designated number of rods and wires, were of the same length. On the top and bottom of the clusters were located the standard 10.00 cm (3.94 in.) long by 1.49 cm (0.588 in.) diameter molybdenum reflector cylinders. As a result of the limited amount of Nb-1Zr tubing available, 12 elements in the buffer region were constructed of aluminum tubing identical to that used in the driver region that will be described below. These elements, however, contained the same fuel and material quantities and the same reflector configuration as did the Nb-1Zr buffer elements. Table IV delineates the masses of the various materials making up the buffer region and summarizes, by material type, the masses of the materials in the TFE mockups that were previously discussed.

#### D. Thermionic Mockup Buffer Region

##### (2) Accuracy of the Buffer Region Simulation

The volume fractions obtained in the buffer region mockup, Figure 9 are compared to the volume fractions specified for the reference design in table II. It is noted that the buffer zone is a close homogeneous approximation to the reference core for all the important materials.

#### E. Driver Region

The remainder of the thermionics core (the driver region) contained pin-type elements identical in overall size to the fuel elements used in previous cores (see references 1 and 2) except that aluminum was used as the structural material instead of tantalum. The driver element was comprised of an outer aluminum tube 2.16 cm (0.850 in.) O.D. by 2.11 cm (0.830 in.) I.D. by 59.94 cm (23.597 in.) long. Inside this tube was placed a second, heavy-walled tube that was 2.03 cm (0.800 in.) O.D. by 1.57 cm (0.620 in.) I.D. by 58.08 cm (22.867 in.) long. The heavy-walled, inner tube was centered axially within the outer tube and the excess length of outer tube at each end was used for placement of the standard aluminum end-fittings of the type shown for Types A, B, and C elements in Figure 13. Rod and wire-type fully-enriched uranium fuel was placed within the inner aluminum tube and was restrained at each end by the standard, solid, molybdenum, reflector segments each 10.00 cm (3.94 in.) long. There were a total of 120 driver region elements, 11 of them located in each of three control drums. (See Figure 5). Since the mass of fuel was fixed in the buffer and TFE regions in the manner previously outlined, all fuel adjustments

necessary for criticality were carried out in the driver region. No materials, other than the fully-enriched uranium, were placed within the driver region element. The total masses of aluminum and molybdenum are shown in separately in table IV for the driver region.

A summary of material masses, except that pertaining to the uranium in the driver region, is given in table V for the core and in table VI for the various reflector segments and auxiliary grid plates described previously.

### III. EXPERIMENTAL METHODS

#### A. Introduction

The basic methods for measuring reactivity, critical mass, and power distribution are identical to those employed previously. (See references 1 and 2). Since the fundamental principles involved in the inverse kinetics technique are somewhat lengthy, they will not be repeated here.\* However, brief descriptions of the methods used to obtain some of the other parameters required on this program follow.

#### B. Measurement of Drum Worth

The inverse kinetics technique was utilized in establishing the reactivity worth of single control drums by one or both of two methods. In the continuous drive method, the reactor was brought to critical, allowed to stabilize, and then the drum was driven from the full-in to the full-out position. The ensuing power trace was analyzed by the inverse kinetics technique in order to derive the worth of the drum as a function of time. From the known drive speed, the worth was then established as a function of position. This continuous drive method was employed to evaluate the worth of a single drum where detailed information on the shape of the worth curve at or near the full-in position was particularly important.

The stepwise method for obtaining the worth of single drums was utilized where greater precision is required at or near the full-out position. The stepwise method involves only small reactivity changes; consequently, the validity of the results is less subject to error. In this technique, Drum No. 6, for example, is placed with fuel full-in and another remotely located drum (No. 4 example) is banked out such that, with all other drums full-in, the reactor is critical. After a period of time is allowed at level power, data collection is initiated, Drum No. 6 is then turned out a few degrees and maintained at that position

---

\*  
Reference 3.

for about one minute. Drum No. 4 is then turned in by an amount that not only offsets the small negative reactivity produced by Drum No. 6, but also provides a small amount of excess. Again, all drums remain stationary for about one minute, whereupon Drum No. 6 is turned out a few degrees more. Drum No. 4 is then moved in and the process is repeated in this stepwise fashion, the worth of Drum No. 6 being measured as it is stepped out and the worth of Drum No. 4 as it is stepped in. The integral worths are established by algebraically summing the stepwise reactivity values. This procedure assumes no interaction between drums, a phenomenon that is less likely to be met in this core configuration than in previous ones.

#### C. Measurement of the All-Drums-In Excess Reactivity

The measurement of the all-drums-in excess reactivity was accomplished in most cases by noting the position of one or more drums when the reactor is just critical and has remained there several minutes. The previously established drum worth curve was then used to determine the excess reactivity that would be obtained if the drum or drums were turned to the full-in position. In some cases, where the total excess reactivity is sufficiently small, the all-drums-in excess reactivity was determined directly to actually driving all drums full-in and analyzing the power rise by the inverse kinetics technique.

#### D. Measurement of Critical Mass

The value for the critical mass of the various core compositions were based upon the all-drums-in excess reactivity value and upon the core-averaged worth of fuel in the driver region only. The latter quantity was determined by noting the change in the all-drums-in excess reactivity that occurred upon removal of uranium fuel from the driver zone in a uniform manner.

#### E. Measurement of Power Distribution

The power distribution in TFE No. 1 was measured by irradiating the foil and punching out rectangles 0.254 cm (0.10 in.) wide by 1.27 cm (0.501 in.) wide at the appropriate places. The rectangles were weighed to an accuracy of  $\pm 0.1$  mg.

The rectangles were counted in several gamma channels beginning a few hours after reactor shutdown. Standard NaI scintillation detectors were used, with the amplifiers set for integral counting of gamma rays above 0.5 Mev. One of these channels was employed to determine the decay "constant" for the rectangles. A least-squares fit of the data for this

curve was used for decay correction. All channels were controlled by the same time base and dual preset counter. Fifteen-minute counting intervals were used, but some wire segments were counted more than once. The channels were normalized to one another by counting a group of several rectangles in all channels and comparing the resulting decay-corrected counts.

A computer code was used to correct the data for decay, background, mass normalization and counter normalization. The resulting relative activities, which are directly proportional to power, were plotted as a function of radial and angular position in the TFE. The errors due to counting statistics only vary from 1/2 to 1-1/2 percent. The mass determination introduced an error of approximately  $\pm 0.2$  percent.

#### F. Units of Measure

All of the reactor component were designed, built, and checked to physical dimensions in inches. Consequently, the International System of Units used here for the unit of length is derived from the latter data. The masses quoted herein for fuel and other reactor materials were, however, measured directly in grams. All other physical units of measurement, unless otherwise noted in the text, were based directly upon the units quoted.

### IV. EXPERIMENTAL RESULTS

#### A. Excess Reactivity

With 4.370 and 24.209 kg of uranium already in the TFE and buffer regions, respectively, the initial fuel loading in each of the 120 driver elements consisted of seven (7) uranium rods each 0.432 cm (0.170 in.) in diameter by 37.51 cm (14.767 in.) long and weighing 102.42 gms. In the 1/M approach-to-critical Figure 14 it was found that the reactor would be substantially subcritical. The loading in each element was therefore increased in a step-wise fashion until eight (8) uranium rods and six (6) uranium wires (each 0.153 cm (0.060 in.) by 37.47 cm (14.75 in.) long) were installed. By the time criticality was reached a total of 136.106 kg, of uranium had been loaded, a value which includes all regions of the reactor.

With a uranium mass loading of 107.527, 24.209 and 4.37 kg in, respectively, the driver, buffer and TFE regions (136.106 kg total) an excess reactivity of  $36.2\%$  was determined by two period measurement. The initial critical position for drum No. 6 was  $31^{\circ}35'$  with drums 4 and 5 full-in. A period of 39.7 sec (corresponding to  $18.8\%$ ) was observed when drum 6 was driven from  $31^{\circ}35'$  to  $21^{\circ}0'$ . Drum No. 4 was then driven



out to maintain level power. Subsequently, drum No. 6 was driven full-in, whereupon a 44.2 sec period (corresponding to 17.4  $\beta$ ) was observed. Thus an all-drums-in excess reactivity of 36.2  $\beta$  was determined for the uniformly loaded driver region and with no teflon in the buffer region.

A total of 9.104 kg of teflon, in the form of 0.152 cm (0.060 in.) thick strips, was added to the buffer region of the core in the locations shown in Figure 15. This material increased the excess reactivity to 79.3  $\beta$  as determined by two similar period measurements and the previous data. The reactor was critical with drum 6 at 49°55' and drums 4 and 5 full-in. A period of 40.5 sec (18.5  $\beta$ ) was observed when drum No. 6 was positioned at 43°, and a period of 25.0 sec (24.6  $\beta$ ) was observed with drum No. 6 at 31°35' and drum No. 4 banked out. These data points, when added to the previous information, indicate a total excess of 79.3  $\beta$  (all-drums-in-excess). The teflon is therefore worth approximately 43.1  $\beta$ .

#### B. Critical Mass

In order to determine a critical mass value, one uranium wire (0.152 cm diameter) was removed from every other fuel element in the driver region only. This removal process resulted in a reduction of 0.76586 kg in uranium mass. With the teflon still in place, two period measurements were again made. In the first, drums 4 and 5 were full in, and drum No. 6 was driven from a critical position of 28°20' to a position of 13°. A period of 32.0 sec was observed and corresponds to an increase in reactivity of 21.3  $\beta$ . Drum No. 4 was subsequently banked out to bring the excess reactivity to zero, whereupon drum No. 6 was driven full-in. A 137 sec period corresponding to a reactivity change of 7.5  $\beta$  was observed. Thus, the all-drums-in excess reactivity was determined to be 28.8  $\beta$  a decrease of 50.5  $\beta$  relative to the previous value. The worth of fuel is therefore 65.94  $\beta$ /kg. An excess reactivity of 79.3  $\beta$  would correspond, consequently, to 1.2028 kg and critical mass of 134.903 kg with teflon strips in place. A critical mass of 135.558 kg is derived for the case without the teflon strips.

#### C. Drum Worth

The reactivity worth of drum No. 6 was measured from full-in to full-out by the inverse kinetics method and the results are shown in Figure 16.

#### D. Power Distribution

##### (1) Foil Counting

The power distribution in a  $U^{235}$  coil foil in TFE Mockup No. 1

(see Figure 15) was determined as a function of radial position along twelve (12) angular positions at the coil midplane. The results are shown graphically in Figures 17, 18, 19, and 20 and are tabulated in table VII. In each of these figures, the relative activity is plotted along a specified angular position as indicated in Figure 15, which is a top view of the core. The ring number refers to the number of turns in the coil, ring number one representing the first turn on the outside of the coil, ring number two the second turn, etc. There are 43 rings, the rings being numbered sequentially as one proceeds inward along the  $0^\circ$  lines. On the outer turn, the end of the foil lies at a point between  $120^\circ$  and  $150^\circ$ . (See Figure 15, which shows a dashed line representing the  $U^{235}$  coil in TFE No. 1). On the inner turn, the end of the foil lies between  $0^\circ$  and  $330^\circ$ .

In order to determine the axial distribution of the power in the coil, foils were punched from positions above and below the midplane at the 0, 180, 240, 270, and  $330^\circ$  angular positions. Table VIII shows the results of these measurements. It is noted that the axial power distribution is relatively flat.

The twelve foils on the inner turn and the twelve foils on the outer turn were counted with one side toward the NaI detector and then with the other side toward the detector in order to determine whether or not there was a significant variation across the foil itself. These results are given in table IX and show the comparison of activities on the inner and outer faces. The term "inner face" refers to that portion of the coil facing the cylindrical teflon rod inside the coil. Except where noted otherwise, all foils were counted with the inner face toward the detector.

Figure 21 is a plot of the relative activity of the coil as a function of angular position for the outer, inner, and tenth turns.

For purposes of dimensional correlations, the inside diameter of the tungsten cup in which the coil was placed was measured to be 2.52 cm (0.993 in.) and the thickness of the  $U^{235}$  foil averages 0.0076 cm (0.0030 in.).

## (2) Film Exposure

After all of the rectangles were punched from the foil, the foil was placed on Type M x-ray film. The film later developed and compared in a rough way with the foil data. In general, the same trends were observed, although the method does not have the resolution inherent in foil counting. The flatness of the axial power distribution was verified by densitometer measurements.

### E. Fuel Element Substitution

In order to determine the effect that the driver region composition has on the power distributions in the TFE, eleven of the  $\text{Ta-Li}_3^{7}\text{N}$  fuel elements used on the previous program were substituted for eleven aluminum type fuel elements in the driver region. No reactivity change was detectable on the basis of drum position.

## V. DISCUSSION OF RESULTS

### A. Experimental

No systematic analytical results that could be used to evaluate the specific degree of accuracy of the experimental values were available. Rough estimates that were carried out to guide the approach to critical indicated a critical mass of the order of 129 kg, a value in reasonably good agreement with the experiment. The less precise data obtained from the inverse multiplication measurements also tend to corroborate the measured critical mass of 135.55 kg that applies to the case in which no teflon is present in the core.

With reference to the reactivity worth of drum No. 6, there is excellent agreement from fuel full-in to about 50 degrees of arc between the period measurements made to determine the small excess reactivity states and the inverse kinetics data. This agreement lends confidence in the accuracy of the drum worth data, at least near the fuel-full-in position.

The power distribution information appears to be reasonably good. The fact that the peak power occurs at the  $330^\circ$  azimuthal position rather than at the  $0^\circ$  position is, perhaps, to be expected in view of the fact that the center BeO reflector is in direct contact with TFE No. 1 and contributes to the slowing down of fast neutrons. The uncertainty in the relative power data is estimated at  $\pm 1.2$  percent. This value is made up of the following parts: (1)  $\pm 0.75$  percent uncertainty as a result of counting statistics, including uncertainties in monitor and background counts, (2)  $\pm 0.1$  percent uncertainty in foil mass values, (3)  $\pm 0.75$  percent uncertainty as a result of estimated errors in the circumferential location of foils punched from the fully-enriched uranium coil and (4)  $\pm 0.2$  percent uncertainty in decay corrections.

The small-scale replacement experiment in which eleven aluminum-type driver fuel elements were replaced by eleven  $\text{Ta-Li}_3^{7}\text{N}$ -type fuel elements provides some indication, but does not prove conclusively, that the power distribution data are relatively independent of the make-

up of the driver region. This result is an important factor in assessing the validity of the conclusion drawn from the power distribution information.

## V. DISCUSSION OF RESULTS

### B. Analytical

The relative foil activity around and diametrically through the mockup thermionic fuel element coil which simulate the thermionic fuel element stage at the midplane of the core and adjacent to the BeO reflector is shown on table VII. The activity was integrated along each radius using the Simpson One-Third Rule<sup>4</sup>. These results were then summed over all radii and the average activity throughout the coil found. The ratio of the activity at each location to the average activity is the value of the local to average power at that location, and the largest value is the peak to average power for the fuel stage. Figure 22 shows the azimuthal local to average power distribution in the mockup fuel stage in the outermost 0.0076 cm (0.003 in.) layer of U-235 foil. The peak to average power for this fuel stage is 1.99 and occurs at the 330° direction.

## VI. CONCLUSION

The power distribution data measured from this series indicate a peak to average power ratio of two for a mockup thermionic fuel stage located at the midplane of the core and adjacent to the BeO reflector. Since this stage is probably located at the core reflector interface having the largest flux gradient and since a very good simulation of the core-reflector interface and the thermionic fuel element stage was achieved in the experiment, it is believed that a power peaking ratio of this magnitude exists in the reference thermionic reflector region. Therefore consideration of a fuel stage peaking factor of two and its effects on fuel stage performance should be studied in design calculations. Although the scope of this program was limited, studies of the effect of the 0.241 cm (0.095 in.) thick Nb-1% Zr sheet adjacent to the BeO reflector on the power peaking factor would be important to fully understand the power distribution in the mixed spectra core-reflector interface region.

## APPENDIX A

## CHEMICAL IMPURITIES IN CORE MATERIALS

Except as noted previously in this document, the same materials and components were used on this program as were used on the previous programs. The pedigrees on all or most of these parts have thus been provided in references 1 and 2. The following information pertains to the chemical composition and purity of the materials used or fabricated on this program. All Nb-1Zr, BeO and W materials were supplied by NASA as a part of the Contract, consequently no information as to chemical purity was obtained.

<u>Material</u>	<u>Function</u>	<u>Type</u>
Aluminum	Driver region fuel elements	6063-T5
Aluminum	Grid plates	6061-T6
Aluminum	0.102 cm (0.040 in.) thick skin on scammable, center and side reflector canisters	505LH3Y
Aluminum	All other structural material in scammable, center and side reflector canisters	6061-T6 or 2024-TY

The 0.0076 cm (0.003 in.) thick fully-enriched foil used to simulate the UC fuel in a TFE was analyzed for chemical and isotopic content. The following results were obtained from four samples.

<u>Chemical Purity (ppm)</u>						
<u>Sample No.</u>	<u>N</u>	<u>O</u>	<u>H</u>	<u>C</u>	<u>Other impurities</u>	<u>Total impurities</u>
1	259	1693	10	260	598	2820
2	183	953	9	310	525	1980
3	433	1877	13	360	556	3239
4	192	1515	12	200	590	2409

<u>Isotopic Purity (%)</u>				
<u>Sample No.</u>	<u>U-234</u>	<u>U-235</u>	<u>U-236</u>	<u>U-238</u>
1	1.134	93.199	0.260	5.407
2	1.136	93.189	0.260	5.415
3	1.135	93.161	0.259	5.445
4	1.122	93.199	0.264	5.417

## REFERENCES

1. Heneveld, W. H.; Paschall, R. K.; Springer, T. H.; Swanson, V. A.; Thiele, A. W.; and Tuttle, R. J.: Experimental Physics Characteristics of a Heavy-Metal-Reflected, Fast-Spectrum Critical Assembly. Rep. AI-71-31, Atomics International (NASA CR-72820), July 30, 1971.
2. Heneveld, W. H.; Paschall, R. K.; Springer, T. H.; Swanson, V. A.; Thiele, A. W.; and Tuttle, R. J.: Experimental Physics Characteristics of a Heavy-Metal-Reflected, Fast-Spectrum Critical Assembly. Rep. AI-72-33, Atomics International (NASA CR-120959), Jan. 28, 1972.
3. Carpenter, S. G.: Reactivity Measurements in the Advanced Epithermal Thorium Reactor (AETR) Critical Experiments. Nucl. Sci. Eng., vol. 21, no. 4, Apr. 1965, pp. 429-440.
4. Kunz, Kaiser S.: Numerical Analysis. McGraw-Hill Book Co., Inc., 1957.

TABLE I  
MASSES OF MATERIALS IN TFE MOCK-UPS (GMS)

TFE No.	Nb-1Zr Discs	† Uranium Foil	Total Uranium	Aluminum* Spacers	Inner* Nb-1Zr Tube	Tungsten Cup	Teflon in W	Teflon* Teflon	Ta Wire	W* ‡ Rods	Outer Nb-1Zr Tube
1	95.46	201.08	1107.93	161.00	170.05	90.10	23.80	101.50	31.07	580.30	1063.05
2	95.46	201.40	1059.22	158.75	169.60	90.30	23.40	101.25	31.00	580.30	1048.30
3	95.46	202.65	1101.43	157.09	169.28	93.70	23.75	107.45	30.83	580.30	1065.25
4	95.46	197.10	1101.31	144.70	168.95	89.61	23.48	119.30	30.42	580.30	1068.05
Total	381.84	802.23	4369.89	621.54	677.88	363.71	94.43	429.50	123.32	2321.20	4244.65

\* Sum of weights of these materials above and below tungsten cup

‡ Based on a measured average of 48.36 gms for each 15.24 cm (6.00 in.) long rod

† Based on a measured average of ten discs

TABLE II  
COMPARISON OF THE VOLUME FRACTIONS OF THE CRITICAL EXPERIMENT  
WITH THERMIONIC REACTOR DESIGN VALUES

	<u>Volume Fractions %</u>		
	<u>Critical assembly</u>		GGA design (May 2, 1972)
	Core buffer region†	TFE REGION (above and below test stage)	
W	11.52	10.06	10.444
Nb-Zr	23.52	23.60	23.257
Al			5.1278
Ta	.842	.626	.82039
Re			.027716
Mo			.11640
Oy	15.93	16.07	15.91
C(in Teflon)	3*	8.00	9.43

\*As many Teflon strips as can be accomodated were added to the interstices between the buffer region fuel elements.

†Average composition of alphabetically designated fuel elements (figure 2).



TABLE III  
BUFFER REGION LOADING SCHEME

Ele- ment Type	No. of Ele- ments	O.D. of Element		I.D. of Element		Length of Element		Material
		(cm)	(in.)	(cm)	(in.)	(cm)	(in.)	
A	11	1.91	0.750	1.55	0.610	59.94	23.597	Nb-1Zr
AA	5	1.91	0.750	1.55	0.610	59.30	23.347	Nb-1Zr
B*	15	1.91	0.750	1.59	0.625	59.94	23.597	Nb-1Zr
C	8	2.22	0.875	1.74	0.685	59.94	23.597	Nb-1Zr
S	12	2.16	0.850	1.57	0.620	59.94	23.597	Al

\* Type B elements actually consist of two tubes, one inside the other. The outer tube is 1.91 cm (0.750 in.) O.D. x 1.73 cm (0.680 in.) I.D. x 59.94 cm (23.597 in.) long, and the inner tube is 1.69 cm (0.665 in.) O.D. x 1.59 cm (0.625 in.) I.D. x 58.10 cm (22.875 in.) long.

#### NOTE

All five types of elements each contain the following:

- 1) Four fully enriched uranium rods each 0.432 cm (0.170 in.) in diameter x 37.49 cm (14.76 in.) long
- 2) Five fully enriched uranium wires each 0.152 cm (0.060 in.) in diameter x 37.47 cm (14.75 in.) long
- 3) Three tungsten rods each 0.457 cm (0.180 in.) in diameter x 37.47 cm (14.75 in.) long

Seven of every twelve elements contain one tantalum wire 0.279 cm (0.110 in.) in diameter x 37.37 cm (14.75 in.) long.

TABLE IV

MASSES OF SOME OF THE CORE CONSTITUENTS IN THE THERMIONICS  
CRITICAL

Component	No. of Components	Material	Mass (gms)
Type A Fuel Elements (Buffer Region)	11	Nb-1Zr	5,555.58
		Mo	3,936.9
		Fuel	5,221.48
		W	1,311.75
Type AA Fuel Elements (Buffer Region)	5	Nb-1Zr	2,482.73
		Mo	1,789.5
		Fuel	2,373.40
		W	596.25
Type B Fuel Elements (Buffer Region)	15	Nb-1Zr	5,942.96
		Mo	5,368.5
		Fuel	7,120.20
		W	1,788.75
Type C Fuel Elements (Buffer Region)	8	Nb-1Zr	6,294.27
		Mo	2,863.2
		Fuel	3,797.44
		W	954.00
Standard Elements (Buffer Region)	12	Al	2,730.12
		Mo	4,294.8
		Fuel	5,696.16
		W	1,431.00
Standard Elements† (Driver Region)	120	Al	27,301.20
		Mo	42,948.0
TFE	4	Nb-1Zr	5,304.37
		Mo	1,431.6
		Fuel	4,369.89
		Teflon	523.93
		Al	621.54

TABLE IV (cont'd)

Component	No. of Components	Material	Mass (gms)
TFE (cont'd)		W	2,684.91
		Ta	123.32

† No fuel loading is listed since it was varied to achieve criticality.

TABLE V  
SUMMARY OF CORE MASSES (All Regions)

Material	Mass (kg)
Nb-1Zr	25.580
Mo	62.633
Ta (TFE and Buffer)*	1.243
Al	3.352
W	8.767
Teflon (TFE and Buffer)	1.434
Fuel (Buffer)	24.209
Fuel (TFE's)	4.370

\* A total of 29 Ta wires was distributed among the buffer region elements.  
Total mass of Ta in buffer region = 1,119.69 gms.

TABLE VI  
MASSES OF BeO REFLECTOR MATERIALS

Component	No. of Component	Material	Mass (kg)
Scrammable Reflector	1	Al	8.426
Segment No. 1*		BeO	37.168
		Nb-1Zr	1.936
Scrammable Reflector	1	Al	8.434
Segment No. 2*		BeO	37.351
		Nb-1Zr	1.936
Center Reflector	1	Al	0.338
		BeO	1.398
Side Reflector	2	Al	1.648
		BeO	5.127
Auxiliary Grid Plates	2	Al	0.103

\*See Figure 5 for segment locations

TABLE VII  
RELATIVE RADIAL POWER DISTRIBUTION IN TFE NO. 1

Azimuthal Position (Degrees)	Relative Activity									
	Ring No. 1*	Ring No. 2	Ring No. 3	Ring No. 4	Ring No. 5	Ring No. 6	Ring No. 7	Ring No. 8	Ring No. 9	Ring No. 10
0	166,404	152,886	144,172	131,779	125,655	119,500	117,123	112,630	110,131	106,484
30	149,068	138,501	130,097	121,838	116,346	111,330	109,895	105,355	104,828	100,810
60	118,533	112,426	108,311	103,706	99,215	97,296	97,276	92,839	93,016	90,981
90	89,730	89,419	88,132	84,739	83,819	83,581	83,131	81,198	81,986	80,597
120	79,449	79,608	80,874	80,085	80,059	79,710	79,669	78,673	79,568	77,673
150	78,315	78,187	80,570	78,068	78,087	76,987	79,341	79,522	79,331	79,513
180	82,624	81,444	83,047	80,562	79,676	80,044	80,123	79,273	81,307	79,933
210	96,971	95,991	95,247	88,858	88,159	87,594	87,071	85,475	87,032	84,652
240	115,829	108,738	107,043	102,505	99,572	96,514	94,221	93,241	93,052	90,959
270	151,183	134,487	129,503	119,387	117,229	110,918	110,402	106,045	105,682	101,264
300	175,192	161,051	149,449	135,026	130,662	124,028	119,242	116,534	115,109	108,041
330	180,542	163,086	152,448	139,708	132,132	126,102	122,263	116,378	115,180	109,156

	Relative Activity									
	Ring No. 14	Ring No. 18	Ring No. 22	Ring No. 26	Ring No. 30	Ring No. 34	Ring No. 38	Ring No. 42	Ring No. 43	
0	100,204	95,822	91,927	89,386	86,900	85,691	86,545	85,989	86,121	
30	95,641	94,379	90,523	88,366	86,279	85,762	86,953	84,948	85,178	
60	89,050	86,411	84,316	84,979	83,960	82,974	83,499	84,503	84,484	
90	80,902	81,137	80,493	80,275	79,785	80,689	82,014	83,665	83,146	
120	79,460	79,044	79,403	80,900	80,906	80,627	82,574	83,204	84,876	
150	79,012	79,649	80,238	79,458	80,573	79,878	82,053	82,900	82,957	
180	79,643	80,270	79,898	79,916	81,054	80,008	81,621	81,909	84,352	
210	84,249	83,767	82,834	82,576	83,089	81,134	84,630	81,709	83,881	
240	87,735	86,804	85,559	84,427	83,692	83,081	84,802	83,637	82,675	
270	96,786	91,434	90,109	88,311	87,474	86,234	86,296	84,252	84,880	
300	103,479	98,154	94,701	91,539	90,346	88,343	87,788	85,650	85,512	
330	102,947	97,335	93,754	91,759	88,868	88,541	87,575	85,673	87,105	

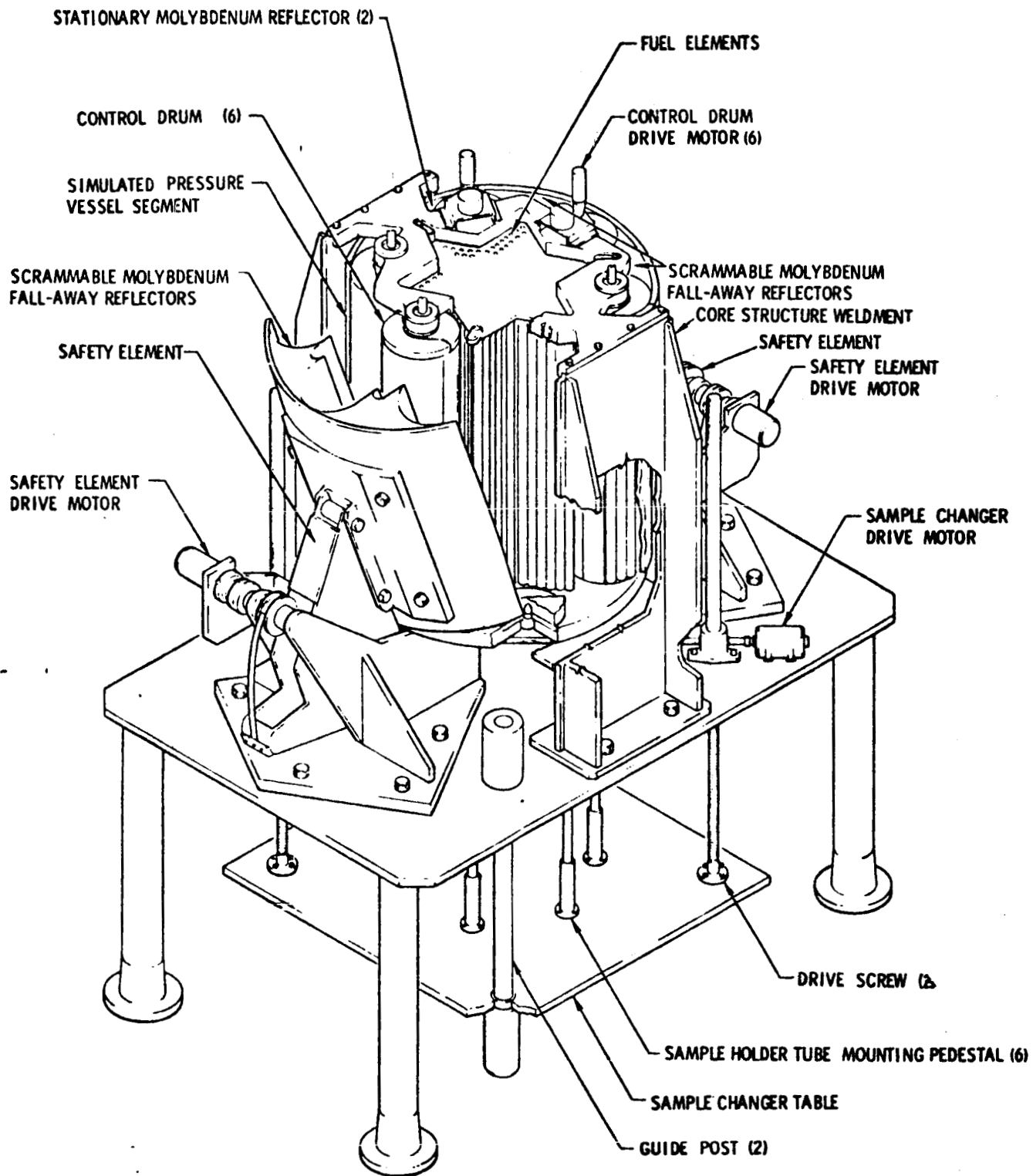
\* The ring number refers to the number of turns in the coil, Ring No. 1 representing the first turn on the outside of the coil, Ring No. 2 the second turn, etc. There are 43 rings if the rings are numbered sequentially as one proceeds inward along the zero degree line.

TABLE VIII  
RELATIVE AXIAL POWER DISTRIBUTION (OUTER TURN)

Angle In Degrees	Relative Activity (Inner Face)		
	Top	Middle	Bottom
0	166,916	166,404	163,885
90	-	89,730	-
180	84,805	82,624	84,117
240	117,014	115,829	-
270	-	151,183	150,862
330	181,329	180,542	184,365

TABLE IX  
COMPARISON OF RELATIVE ACTIVITY  
ON INNER AND OUTER FACE OF FOIL

Position (Degrees)	Relative Activity			
	Outer Turn		Inner Turn	
	Inner Face	Outer Face	Inner Face	Outer Face
0	166,404	166,561	86,121	85,978
30	149,068	148,665	85,178	84,918
60	118,533	120,310	84,484	84,114
90	89,730	90,540	83,146	83,700
120	79,449	79,629	84,876	84,260
150	78,315	78,500	82,957	83,723
180	82,624	82,822	84,352	84,035
210	96,971	97,904	83,881	84,716
240	115,829	117,399	82,675	82,399
270	151,183	153,120	84,880	84,903
300	175,192	177,642	85,512	85,939
330	180,542	180,989	87,105	86,184



6-24-71 UNCL

7765-46068

Figure 1. Sketch of Critical Assembly



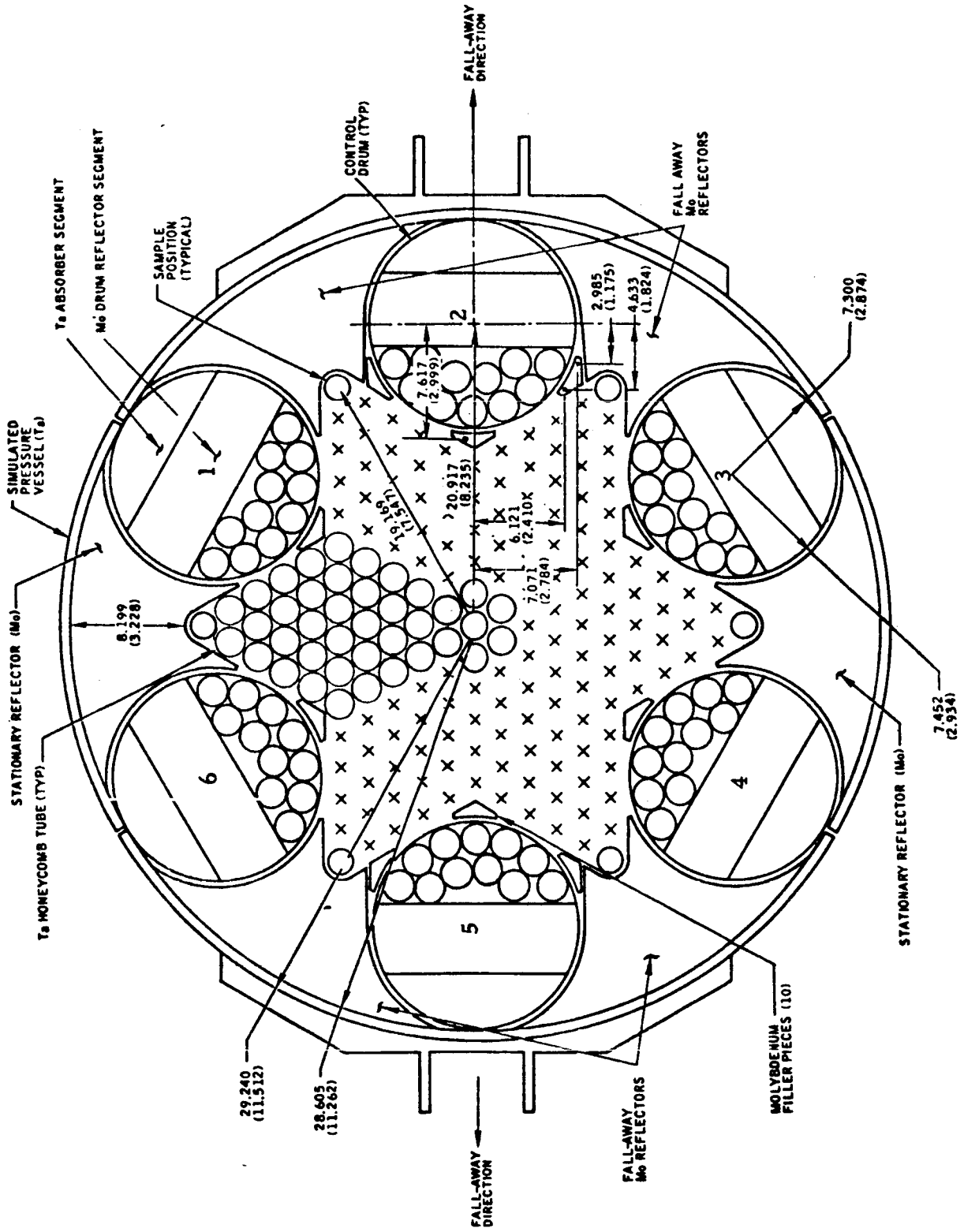
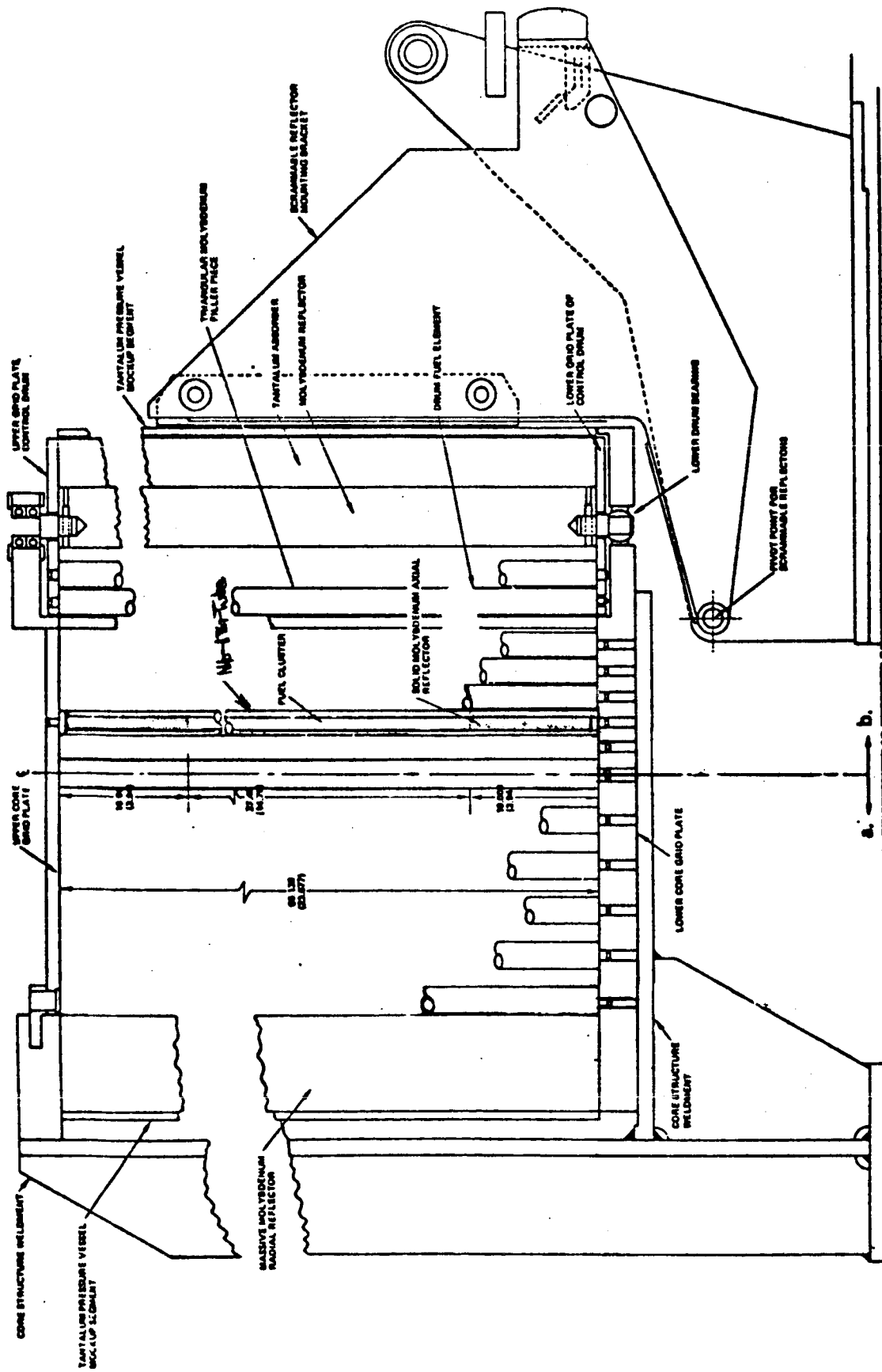


Figure 2. Cross Sectional View of the Critical Assembly at the Core Midplane



7765-4617A

a. Vertical Plane Passing Through the Axis of the Core and the Axis of the Fuel Element at a Point of the Star

b. Vertical Plane Passing Through the Axis of the Core and the Axis of a Drum

Figure 3. Cross Sectional View of the Critical Assembly in the Vertical Direction



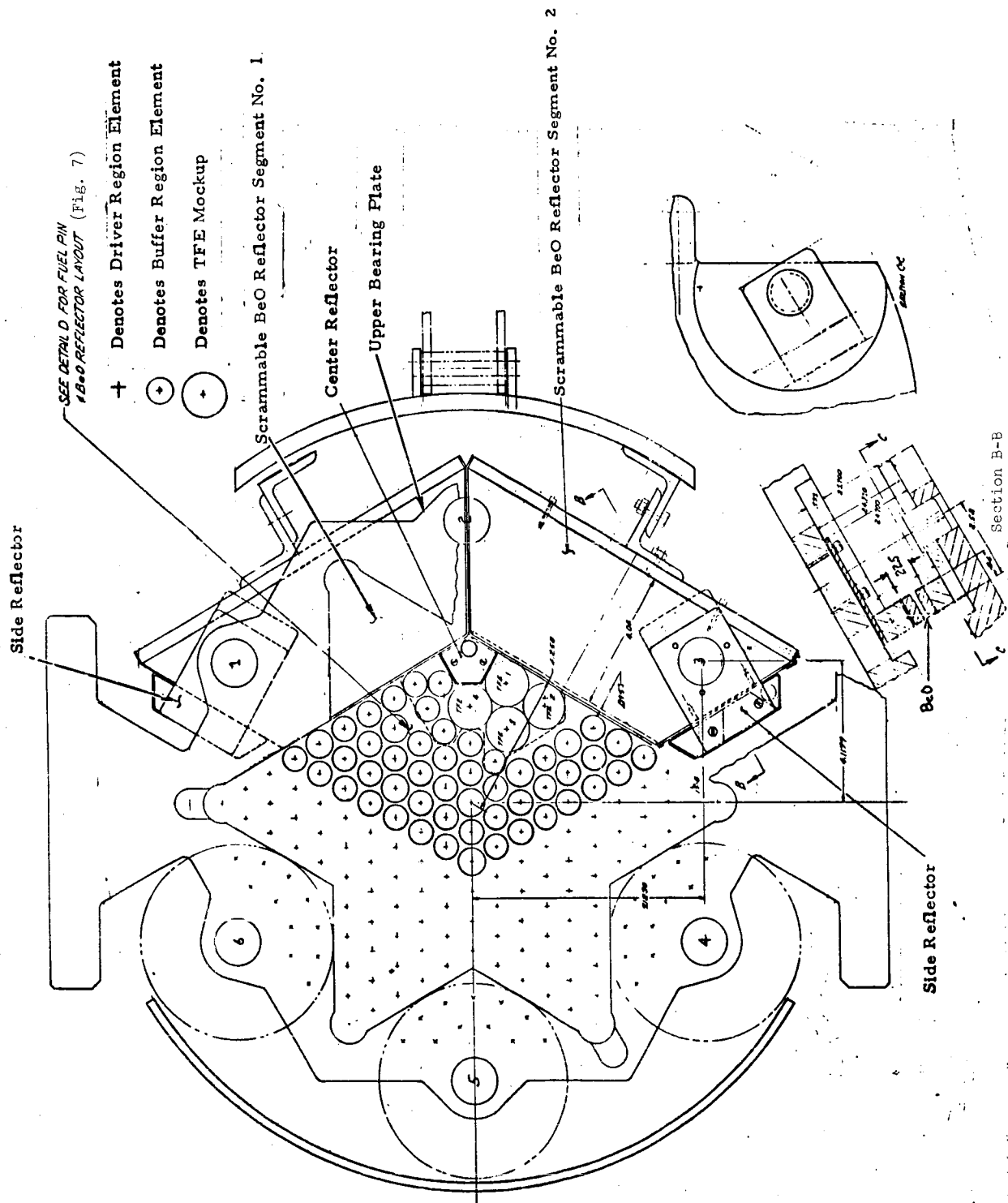
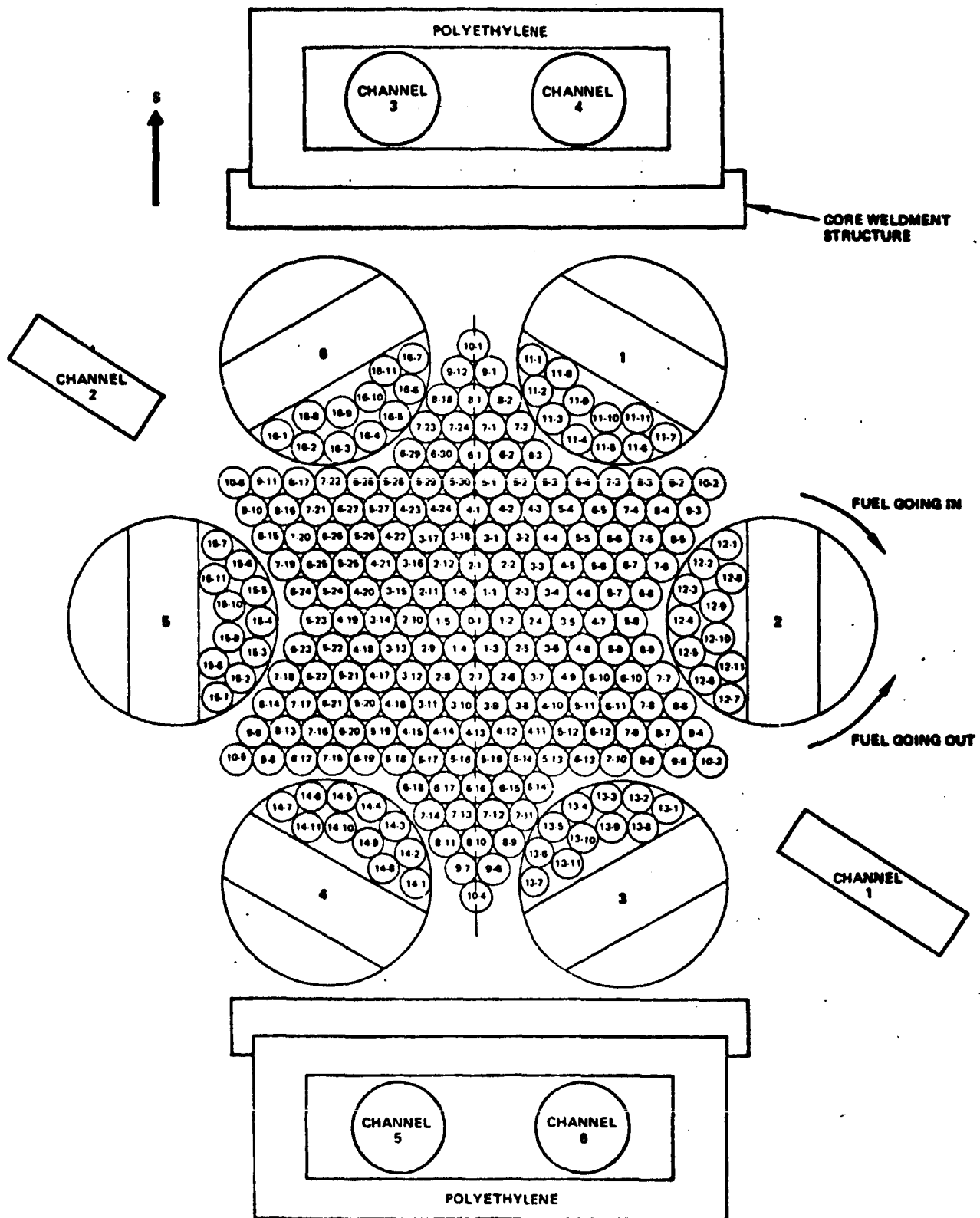


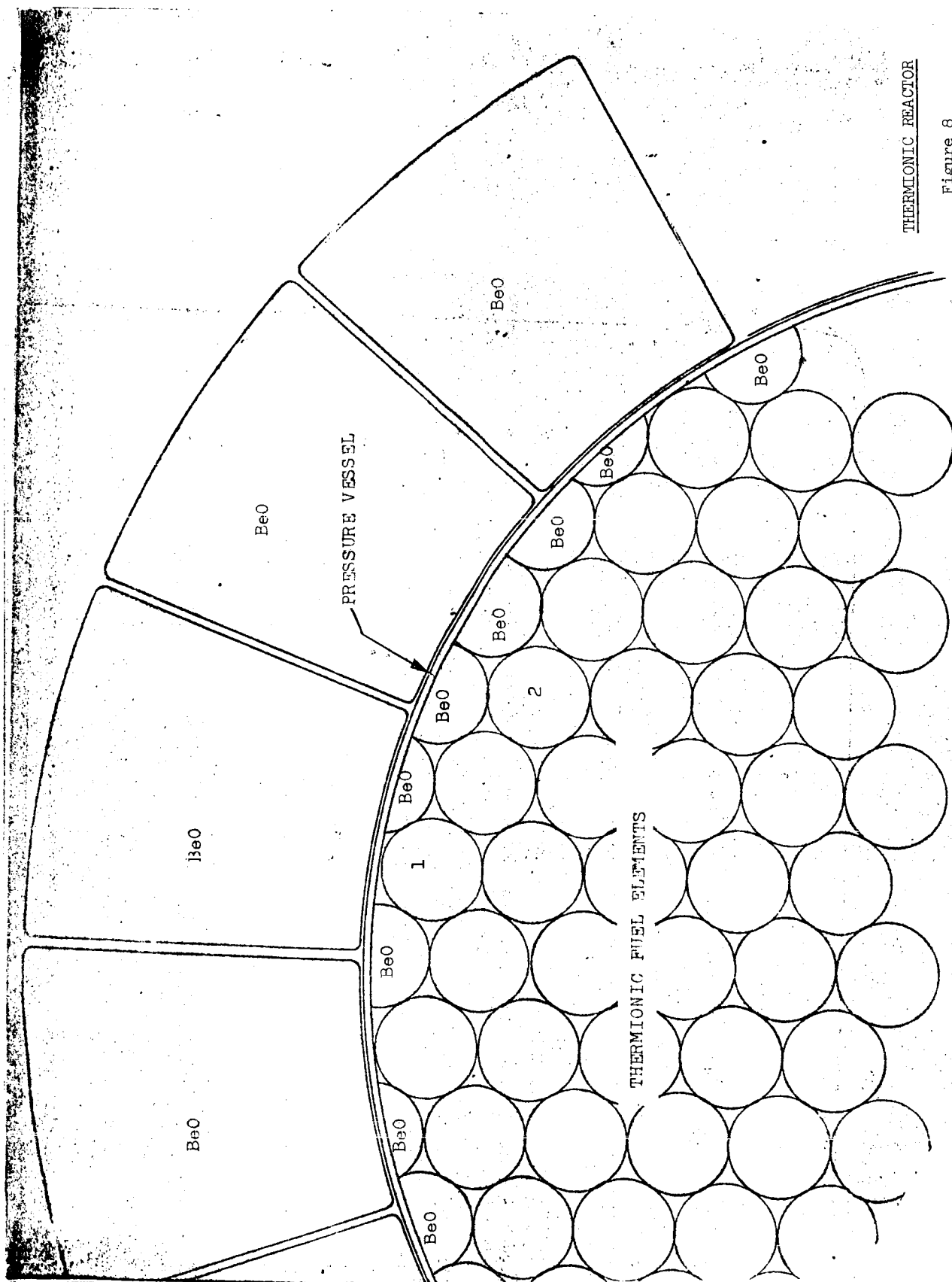
Figure 5. Thermionic Critical Assembly Layout



7705-4631A

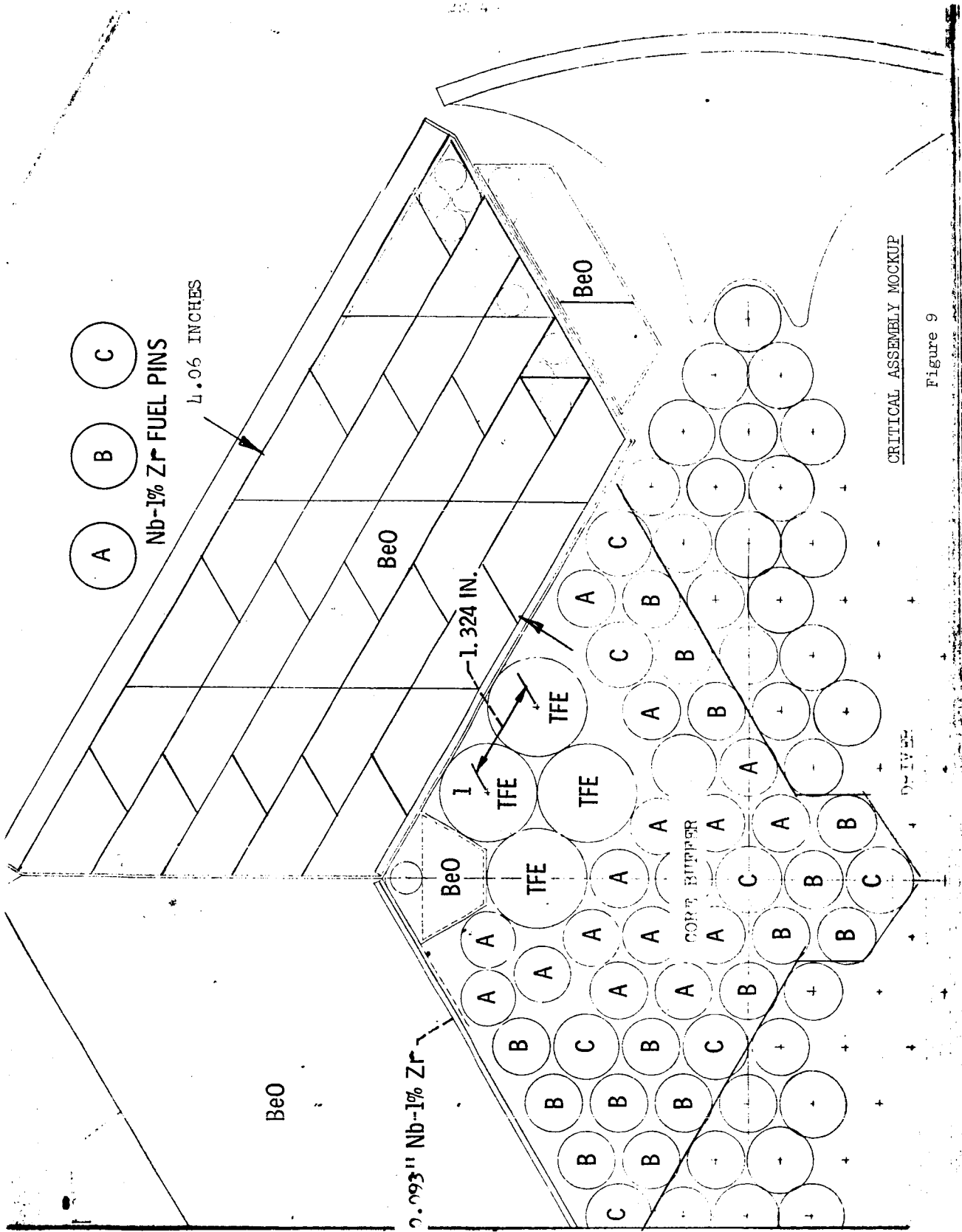
Figure 6 Core Map and Neutron Detector Locations





THERMIONIC REACTOR

Figure 8



CRITICAL ASSEMBLY MOCKUP

Figure 9



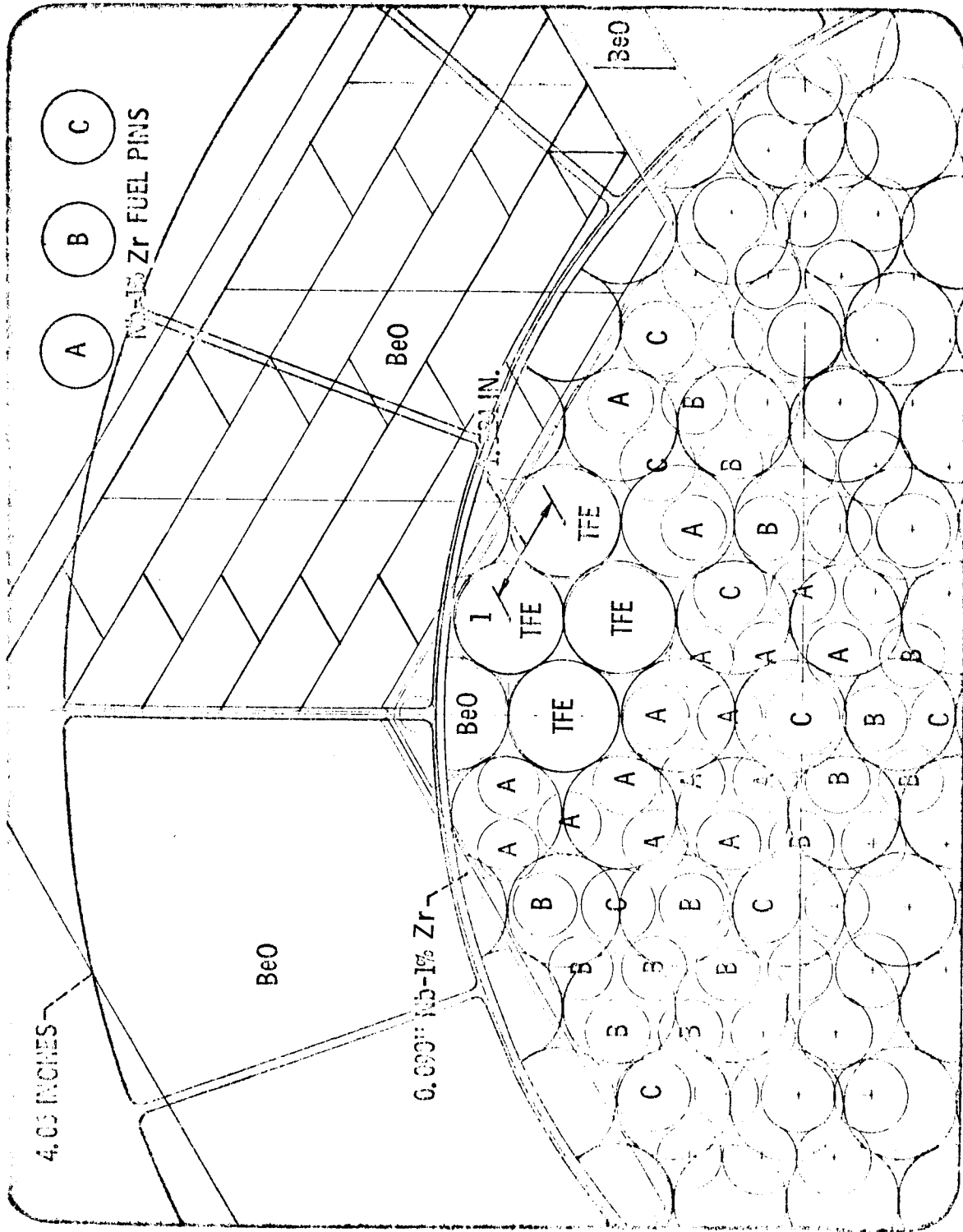
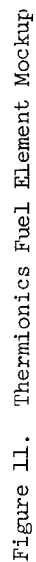


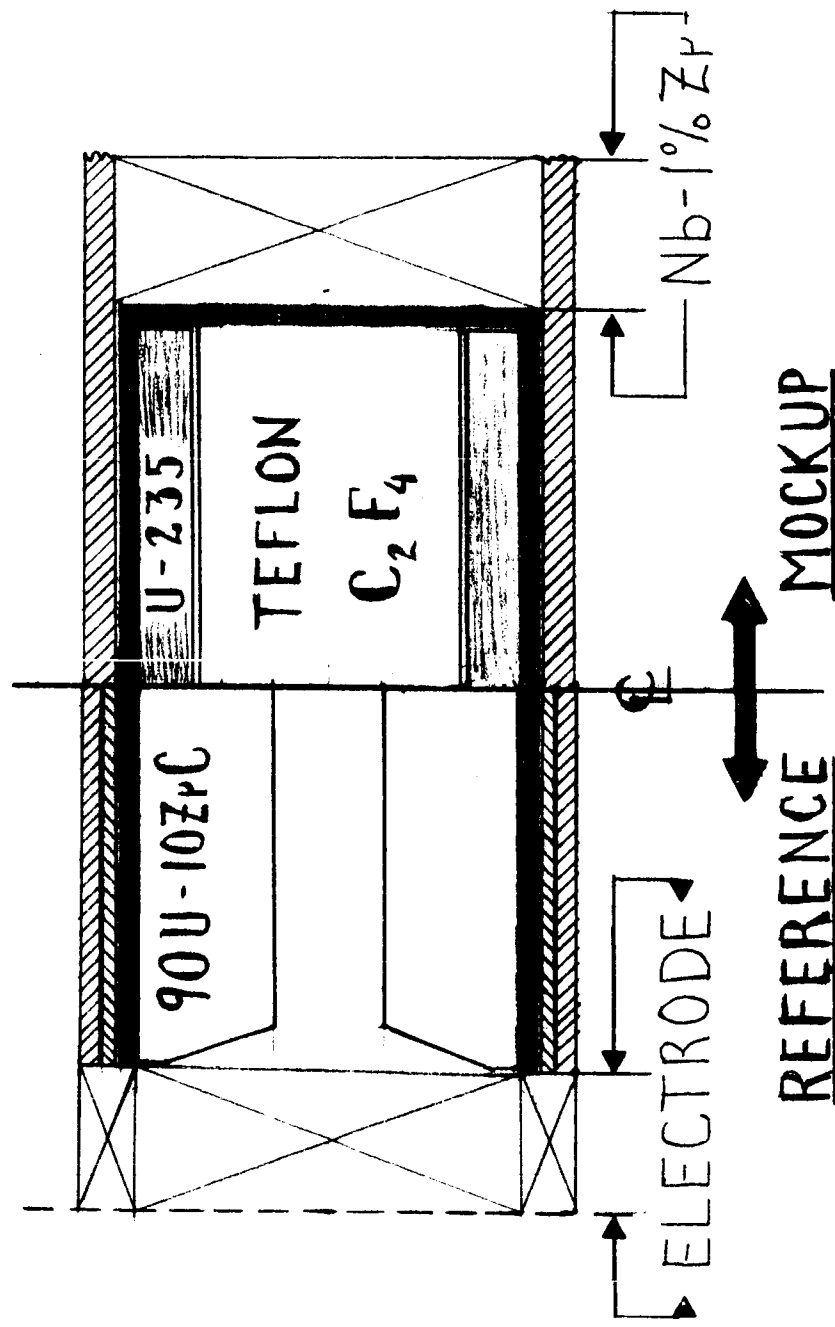
Figure 10.



■ TUNGSTEN

▨ SHEATH Nb-1% Zr

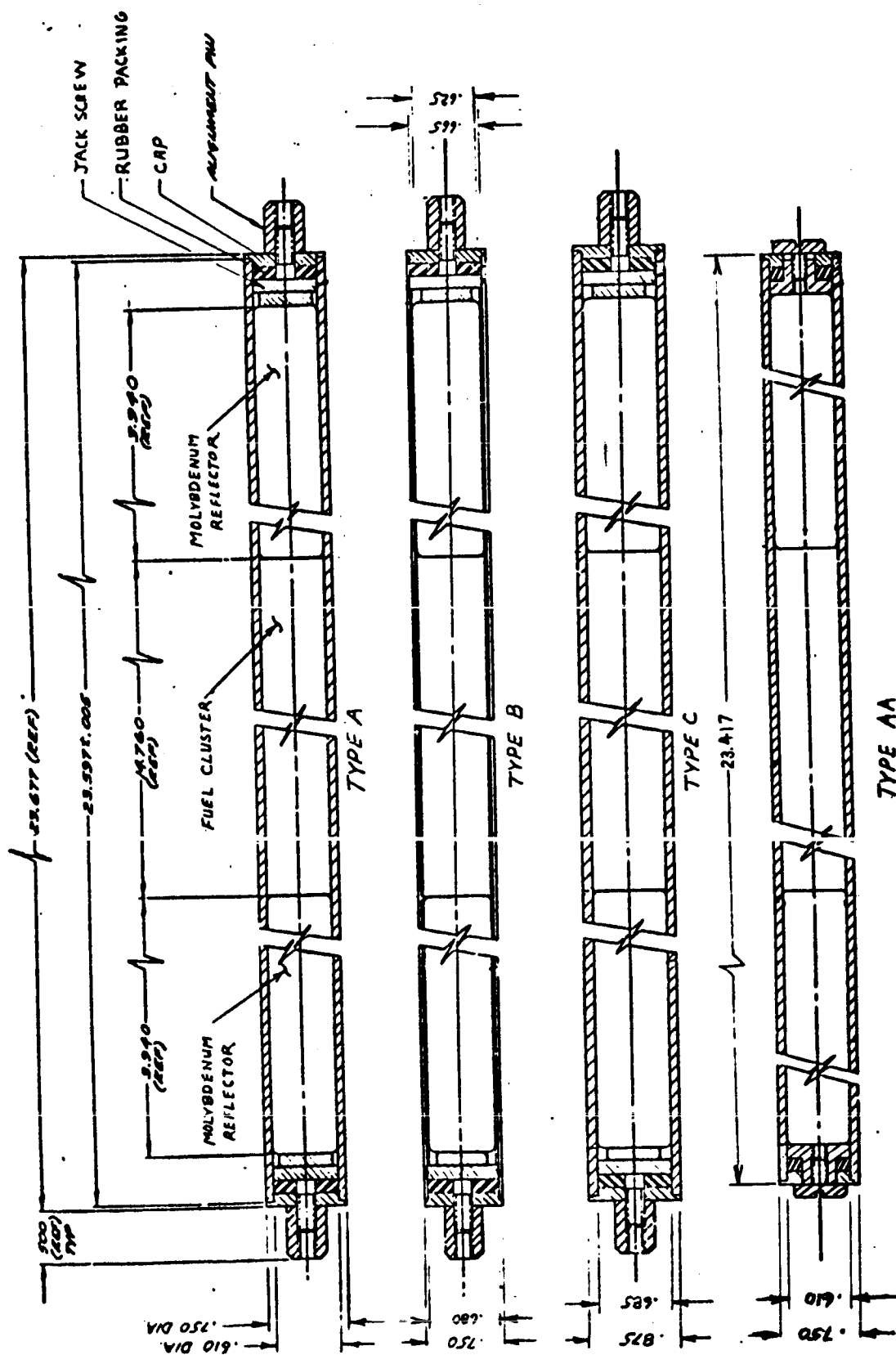
▨ COLLECTOR Nb



## COMPARISON OF MOCKUP AND REFERENCE STAGE

Figure 12.

## BUFFER REGION FUEL ELEMENTS



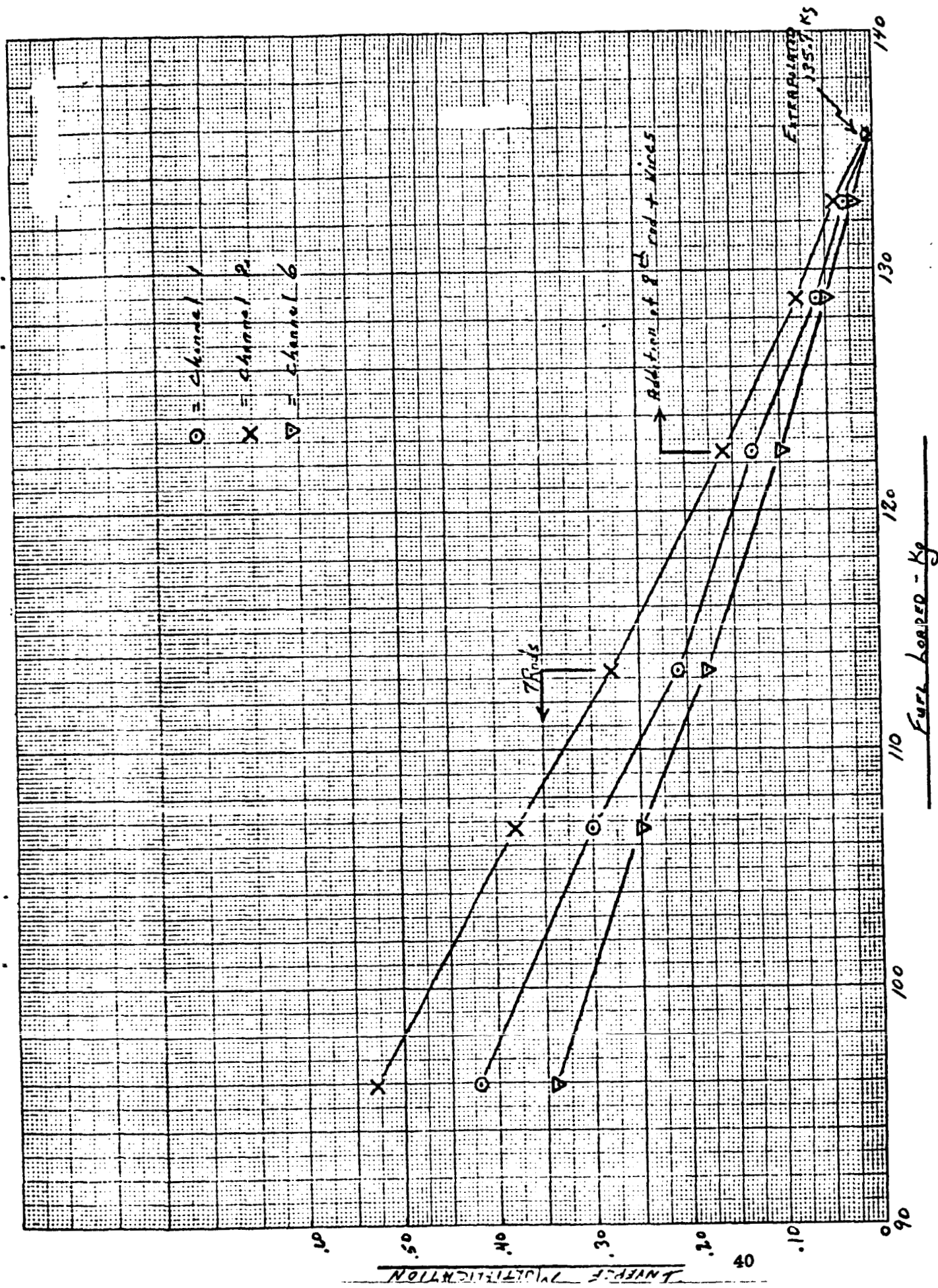


Figure 14. Inverse Multiplication vs Fuel Loading



# Reactivity Worth of Drum No. 6

Thermionics Critical Assembly

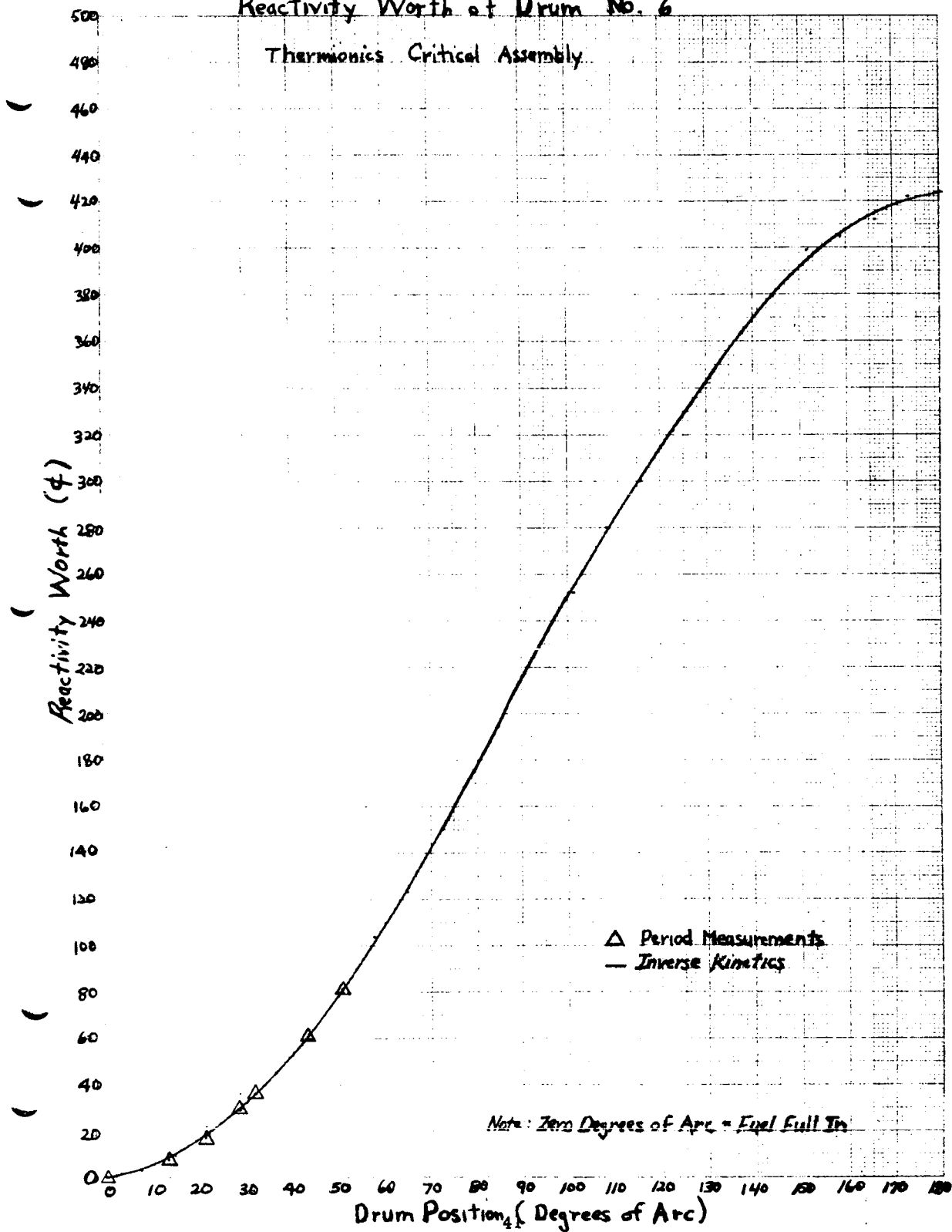


Figure 16.

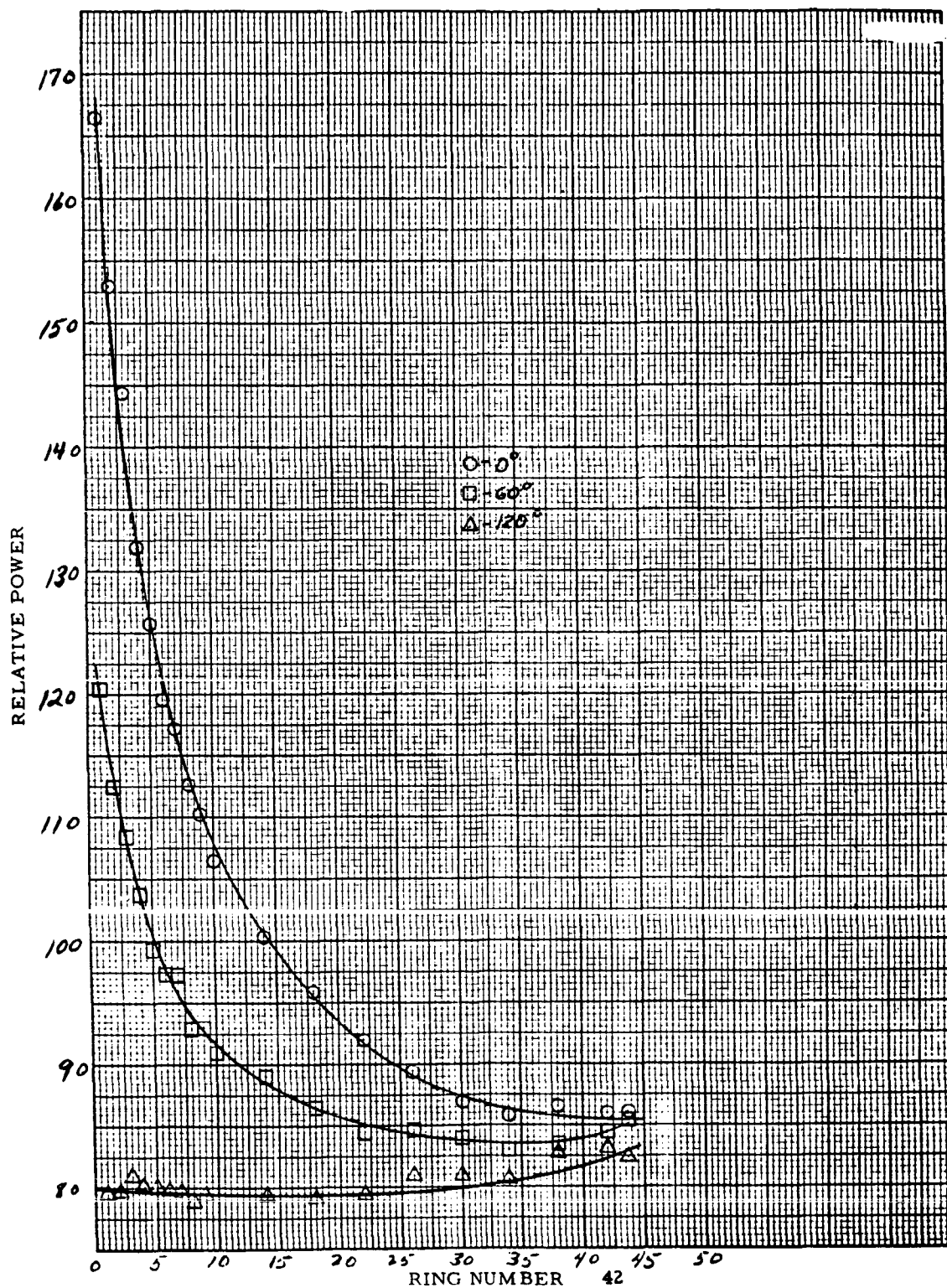


Figure 17. TFE Power Distribution at 0, 60, and 120°



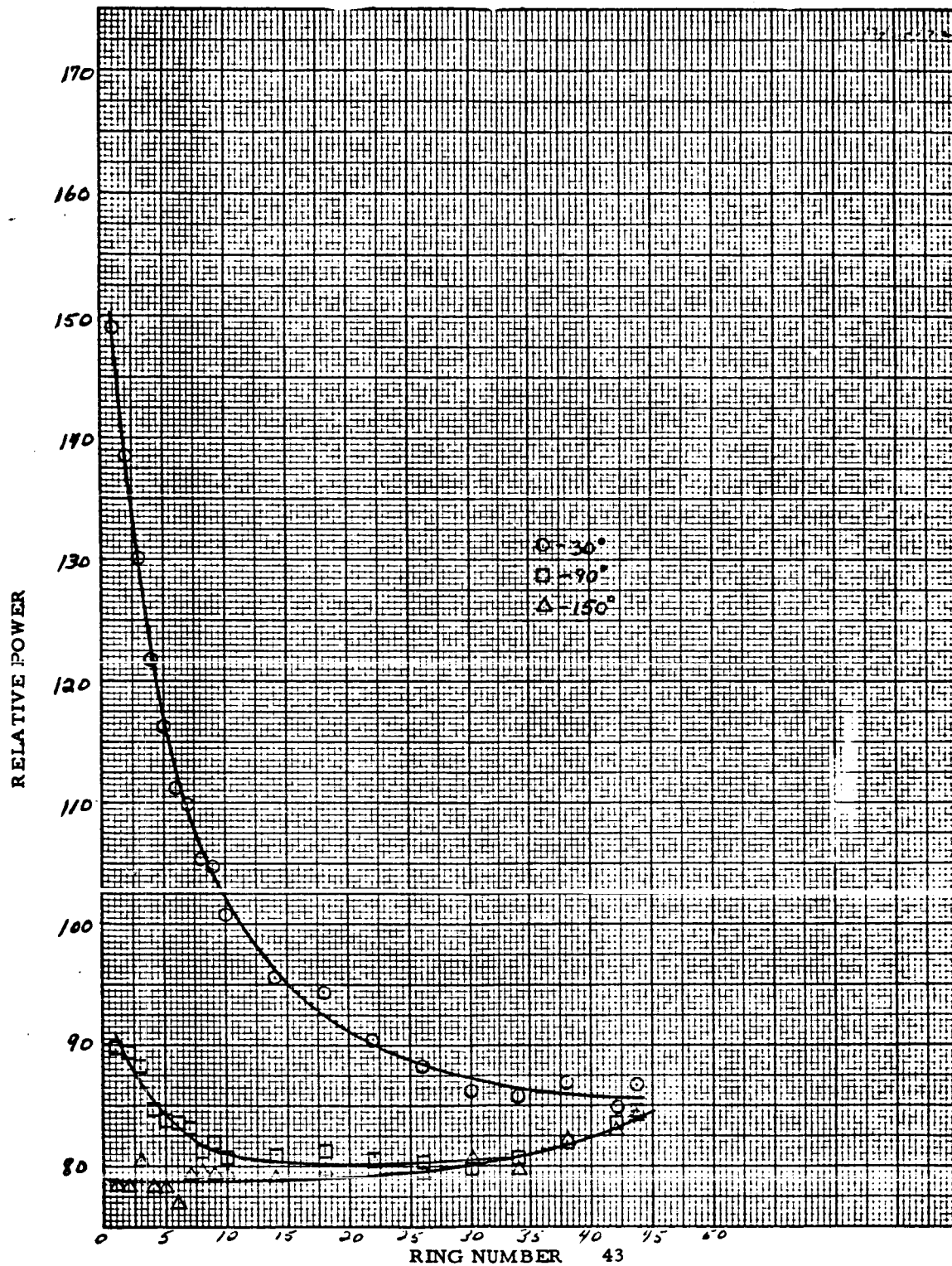


Figure 18. TFE Power Distribution at 30, 90, and 150°

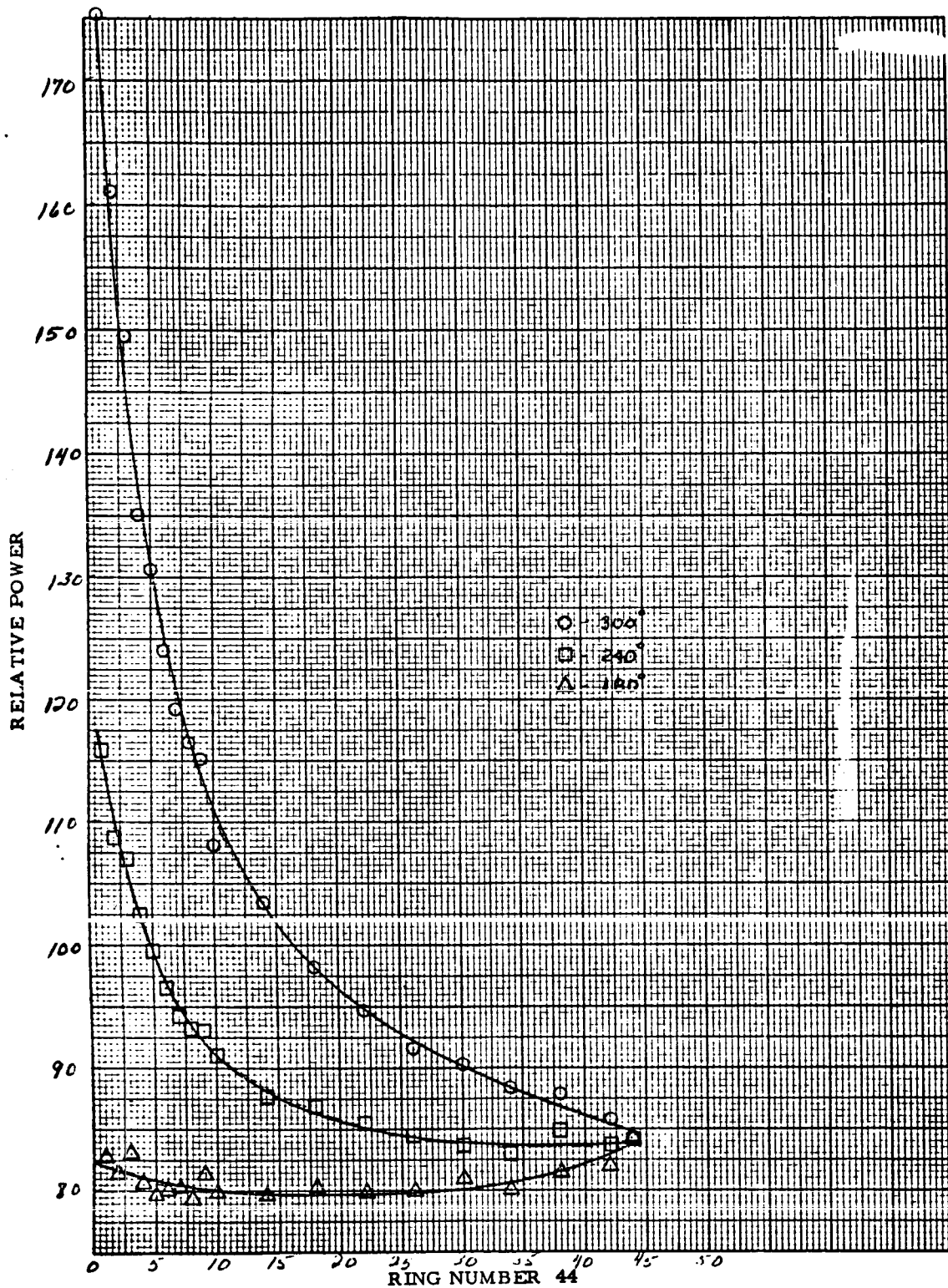


Figure 19. TFE Power Distribution at 180, 240, and 300°

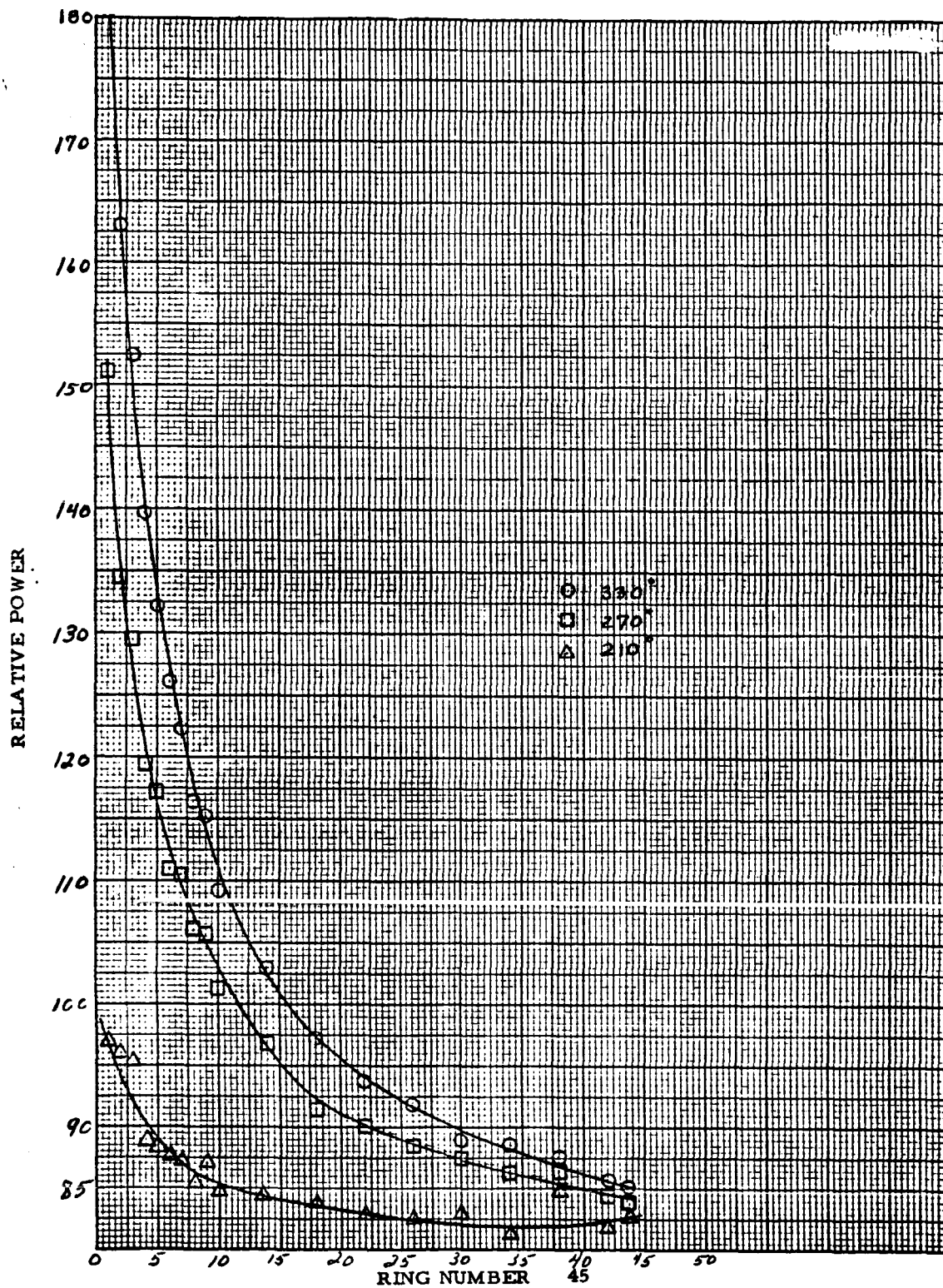


Figure 20. TFE Power Distribution at 210, 270, and 300°

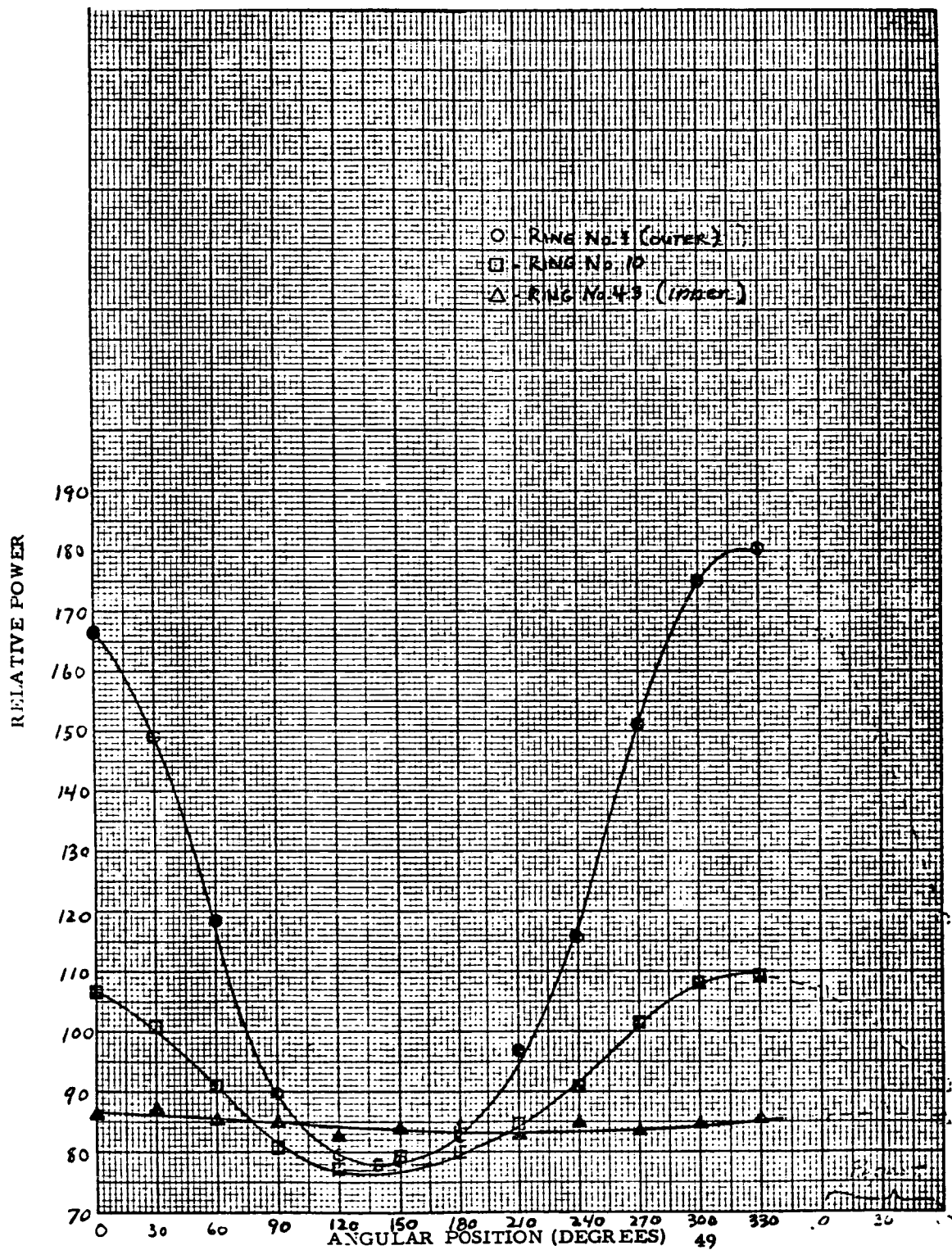


Figure 21. TFE Power Distribution-Azimuthal Plot

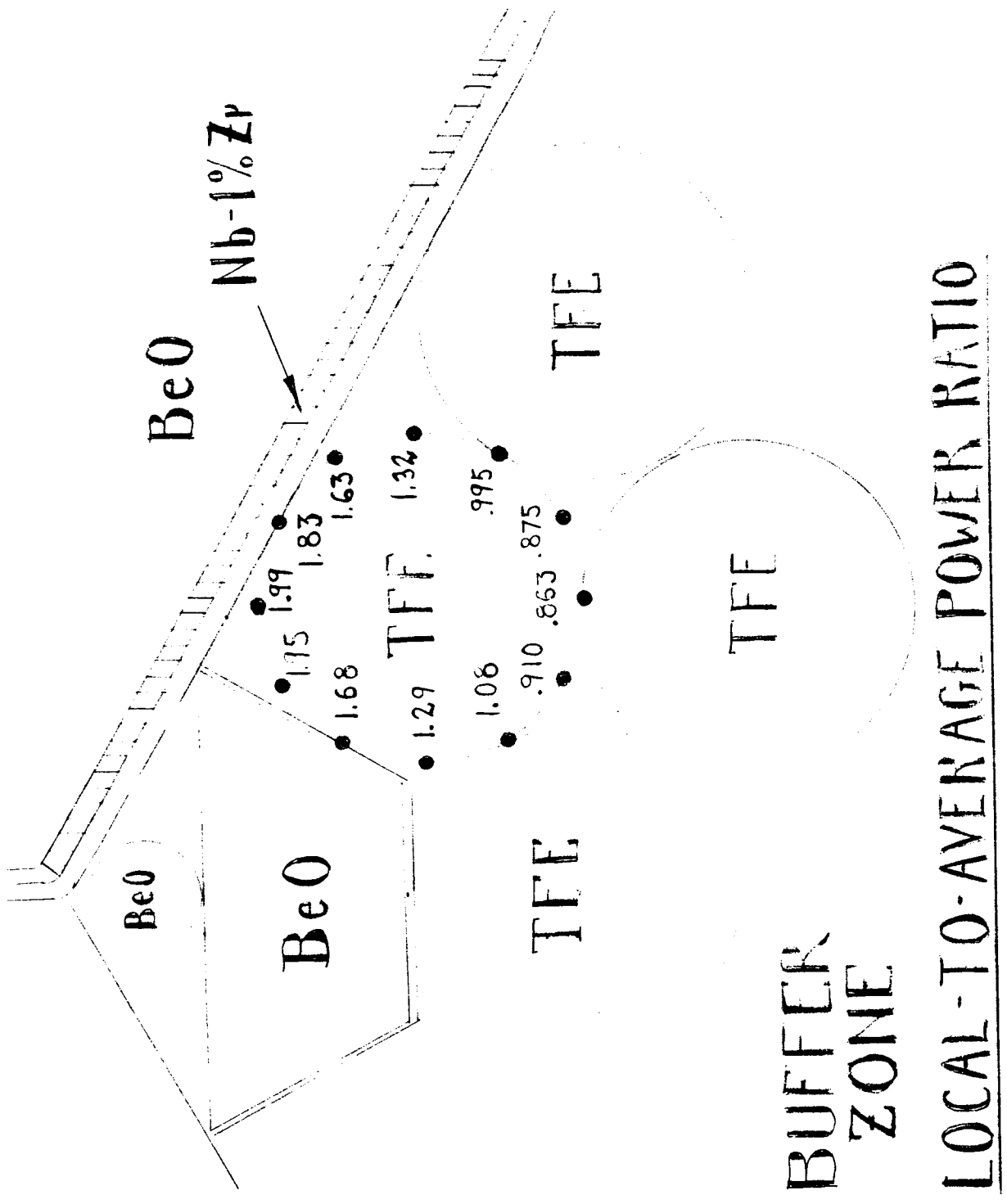


Figure 22.